Article
Vol. 24, No. 6, p. 701–721, December 2020
https://doi.org/10.1007/s12303-020-0005-z
pISSN 1226-4806 eISSN 1598-7477
Geosciences Journal GJ

Scheelite geochemistry of the Sangdong W-Mo deposit and W prospects in the southern Taebaeksan metallogenic region, Korea

Jung Hun Seo[1]*, Bong Chul Yoo[2], Yun-Seok Yang[1], Jun Hee Lee[1], Jaeho Jang[3], and Dongbok Shin[4]

[1]Department of Energy and Resources Engineering, Inha University, 100 Inha-ro, Michuhol-gu, Incheon 22212, Republic of Korea
[2]Korea Institute of Geosciences and Mineral Resources (KIGAM), 124 Gwahak-ro, Yuseong-gu, Daejeon 34132, Republic of Korea
[3]School of Earth and Environment Sciences, Seoul National University, 1 Gwanak-ro, Gwanak-gu, Seoul 08826, Republic of Korea
[4]Department of Geoenvironmental Sciences, Kongju National University, 56 Gongjudaehak-ro, Gongju-si, Chungcheongnam-do 32588, Republic of Korea

ABSTRACT: We compare the trace element geochemistry of scheelite from the economic Sangdong W-Mo deposit with scheelite from unmineralized or sub-economic prospects in Joongdong and Sangdong area in the southern Taebaeksan metallogenic region, to investigate the ore-forming processes controlling scheelite mineralization and to provide a geochemical model for W exploration. In the Sangdong W-Mo deposit, the Mo substitution into scheelite as a powellite ($CaMoO_4$) component changed colors of scheelite fluorescence under short-wavelength UV from yellow (Mo up to 51,000 μg/g) to blue (Mo up to 3.2 μg/g). Low-Mo scheelite with blue fluorescence occurred in the low-grade periphery of the Sangdong deposit and contained higher concentrations of Sr, possibly indicating a lower degree of fluid-rock interaction of the scheelite-forming fluid with Sr-bearing host. Mo-rich scheelite with yellow fluorescence accumulated in the W-rich center of the Sangdong deposit. Hence, the fluorescence color of scheelite reflected both the fluids oxidation state and the degree of fluid-rock interaction and might be useful for scheelite exploration in the Taebaeksan region. In the Sangdong deposit, Nb concentrations in scheelite were high and negatively correlated with its Eu anomaly values, suggesting extensive batholith-scale fractionation in a large magmatic reservoir. Conversely, much lower Nb concentrations of scheelite in the Joondong area suggests a relatively small or isolated magma reservoir that did not reach the same degree of fractionation at the point of fluid saturation, which would limit the potential for an economic scheelite mineralization. Scheelite Nb/Ta ratio is found to effectively differentiate economic orebodies and subeconomic prospects in the Taebaeksan metallogenic region and might be a useful parameter for scheelite exploration.

Key words: Taebaeksan region, scheelite, Sangdong deposit, LA-ICP-MS, geochemical exploration

Manuscript received September 10, 2019; Manuscript accepted January 12, 2020

1. INTRODUCTION

The Taebaeksan region is located in northeastern South Korea and hosts important economic metallic resources of W-Mo-Fe-Zn-Pb and non-metallic resources such as limestone and coal (Kim and Kim, 1978; Yun and Silberman, 1979; Yun and Einaudi, 1982; Yun, 1983; Park et al., 1988; So et al., 1993; Park and Chang, 2005). Metallic ore deposits in the region were mined for W, Mo, Fe, Zn, Cu and Pb from the 1970s (Choi et al., 2009), but few mines now remain operational (Lee et al., 1990; Lee et al., 1996a; Yoo, 2012). However, whereas the number of metallic mines has decreased, mining of limestone and high-Ca marble continues to contribute to the local economy (Noh and Oh, 2005; Kim et al., 2017). Furthermore, recent geological and drilling exploration activities (Chi, 2011; Gliddon et al., 2012; Wheeler, 2016; Yoo, 2016) indicate potential for undiscovered metallic mineral resources (e.g., W, Mo, Cu, Au, Zn and Pb) in the region.

*Corresponding author:
Jung Hun Seo
Department of Energy and Resources Engineering, Inha University, 100 Inha-ro, Michuhol-gu, Incheon 22212, Republic of Korea
Tel: +82-32-860-7557, E-mail: seo@inha.ac.kr

Electronic supplementary material
The online version of this article (https://doi.org/10.1007/s12303-020-0005-z) contains supplementary material, which is available to authorized users.

Scheelite is generally deposited in W deposits by interactions between magmatic-hydrothermal fluids and calcareous rock. Scheelite in some W deposits is enriched during the hydrous-dominated late stages of skarn formation, and is commonly associated with amphibole and mica (Newberry, 1982). While W deposits are dominantly associated with highly fractionated magmas enriched in incompatible elements such as high field strength elements and lithophile elements (Barton, 1987; Audétat and Pettke, 2003; Audétat, 2010; Huang and Jiang, 2014), the geochemistry of hosting lithology during deposition is considered a critical factor for the precipitation of W minerals such as wolframite and scheelite (Polya, 1988; Lecumberri-Sanchez et al., 2017; Seo et al., 2017).

Various trace elements such as rare earth elements (REEs) and high field strength elements substitute into the structure of scheelite formed in hydrothermal ore deposits (Sylvester and Ghaderi, 1997; Ghaderi et al., 1999; Guo et al., 2016; Fu et al., 2017). Trace element analysis of scheelite provides information on fluid compositions and source rock characteristics of hydrothermal mineralizations (Ghaderi et al., 1999; Fu et al., 2017). The shapes of REE patterns and of Eu anomaly values in scheelite are inherited from fluid sources but also reflect physic-chemical conditions present at the time of mineral precipitation (Brugger et al., 2000) including pH and redox change (Ghaderi et al., 1999; Brugger et al., 2008; Fu et al., 2017).

While the trace element concentrations of scheelite provide an invaluable geochemical record of the ore-forming process, no study has yet addressed the possibility of using scheelite chemistry to explore for hidden and potentially economic W ore deposits. Here, we compared the trace element geochemistry of scheelite from sub-economic prospects in the southern Taebaeksan metallogenic region of Korea with that of scheelite from the economic Sangdong W-Mo deposit located in the same region, to evaluate the potential of this approach for exploring undiscovered W orebodies. Based on the results of detailed petrographic analyses of the paragenetic sequence and crosscutting relationships of the Sangdong W-Mo deposit (e.g., fluid inclusion and geochronology; Seo et al., 2017), we applied in situ laser ablation (LA) ICP-MS microanalysis to scheelite crystals from different orebodies in the region. Since scheelite is disseminated and fine-grained in most W-bearing orebodies and prospects in the region, we utilized this in situ analytical technique because of its high spatial resolution.

2. GEOLOGICAL BACKGROUND

The Taebaeksan region consists of Paleozoic basin sedimentary rocks and late Cretaceous intrusives and is divided by the E-W trending Baekunsan (or Hambaek) syncline (Fig. 1) (Hong, 1986;

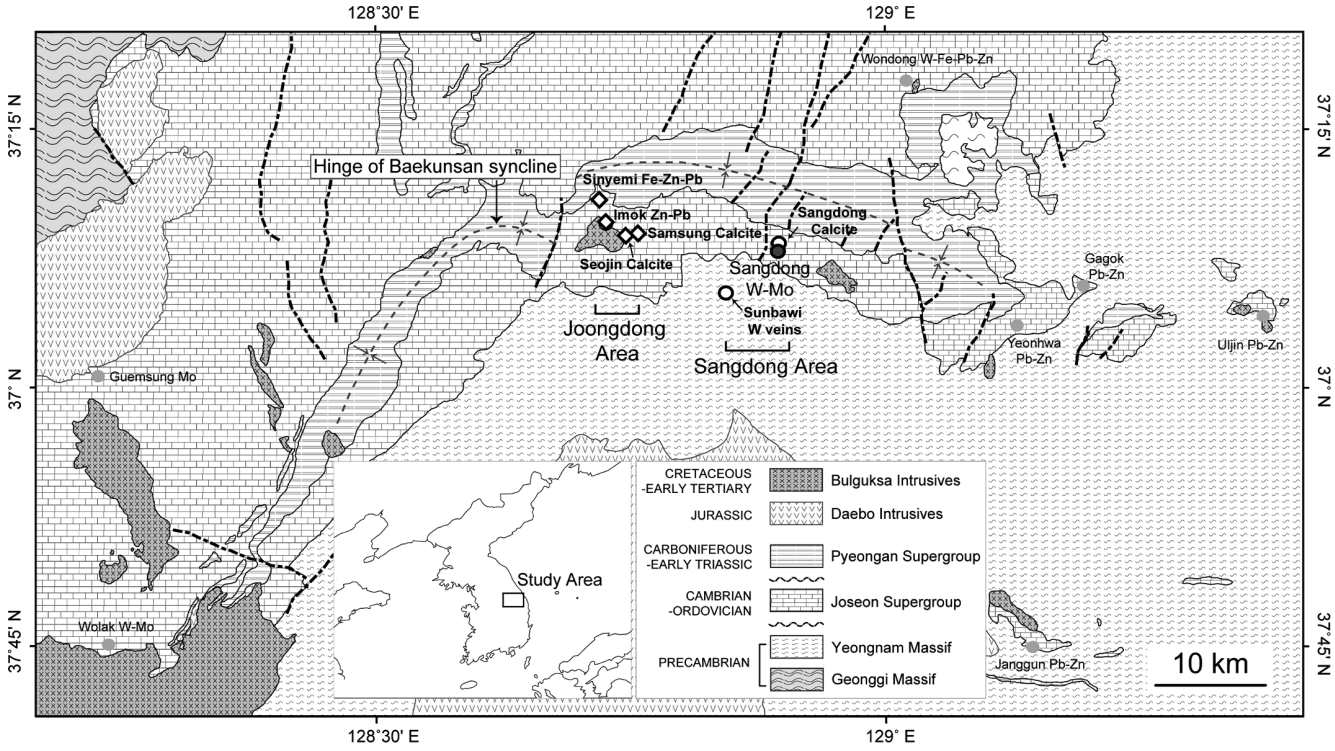

Fig. 1. Geology of the Taebaeksan metallogenic region and the locations of the scheelite-bearing deposits in the southern part of the region. This can be divided north to south about the hinge line of the Baekunsan syncline. The Sinyemi Fe-Pb-Zn skarn deposit, the Imok Pb-Zn skarn deposit, and the Samsung-Seojin calcite marble deposits are located in the Joongdong area, and the Sangdong W-Mo deposit, the Sangdong calcite marble deposit, and the Sunbawi quartz-scheelite veins are located in the Sangdong area. The Sangdong W-Mo deposit is the only economic W deposit in the region. The map is modified after Seo et al. (2017).

Yun, 1986; Moon, 1991a). While some Fe-Pb-Zn-W deposits north of the Baekunsan syncline contain some economic ore deposits (Chang et al., 1995; Hwang and Lee, 1998; Park et al., 2013; Park et al., 2017a, 2017b; Lee et al., 2019), mineral deposits in the southern part of the region, such as the Sangdong W-Mo, Yeonhwa Zn-Pb, and Sinyemi Fe-Zn-Pb deposits (Farrar et al., 1978; Yun and Silberman, 1979; Sato et al., 1981; Kim and Nakai, 1982; Yun and Einaudi, 1982; Moon, 1984a; Koh et al., 1992; Lee, 2001; Choi et al., 2014; Seo et al., 2017) have much higher ore grades and tonnages. Sulfur and Pb isotope studies in the Taebaeksan region (Lee, 2016; Lee, 2018) suggest that contributions of fluids from magmatic source to magmatic-hydrothermal ore deposits in the southern Taebaeksan region are greater than in the northern region. This may be attributed to regional structural configuration, as the southern region is controlled by N-S trending strike-slip faults, whereas dip-slip faults including thrusts are more prevalent in the northern region.

The Sangdong W-Mo deposit is located in the Sangdong area in the SE Taebaeksan region (Fig. 1), and is the largest scheelite deposit in Taebaeksan with 13.3 Mt of probable reserves (0.425% WO_3 and 0.039% MoS_2) (Gliddon et al., 2012). Other smaller scheelite-bearing prospects are located in southern Taebaeksan and include skarn, carbonate-replacement, and vein-type W orebodies. In this contribution we classified groups of scheelite-bearing orebodies and prospects in the southern Taebaeksan region into Joongdong area (SW part of Taebaeksan region) and Sangdong area (SE part of Taebaeksan region). Sangdong W-Mo deposit, Sunbawi veins, and Sangdong calcite deposit are located in the Sangdong area, while Sinyemi deposit, Imok deposit, and Samsung and Sungwoo calcite deposits are located in the Joongdong area.

2.1. The Southern Taebaeksan Metallogenic Region

Precambrian metamorphic complexes of the Yeongnam Massif form basement lithologies in the Taebaeksan metallogenic region (Gaudette and Hurley, 1973; Moon, 1987; Yun, 1988; Park et al., 1993) (Table 1 and Fig. 1). The Precambrian basement comprises meta-granitic and meta-sedimentary rocks, unconformably overlain by early Paleozoic carbonate-rich rock of the Joseon Supergroup (Choi, 1998; Kim and Lee, 2000; Lee and Lee, 2003). The Cambrian–Ordovician Joseon Supergroup is composed of several sedimentary formations (Jangsan quartzite, carbonate-rich Myobong slate, Pungchon limestone, shale-carbonate interlayered Hwajeol limestone, Dongjeom quartzite, Dumudong shale, and Maggol limestone; Table 1). The majority of metallic ore and limestone deposits in the Taebaeksan region are hosted in sedimentary rocks of the Joseon Supergroup (Park et al., 1988), and the most important are several carbonate-rich layers in the upper part of the Myobong slate and lower part of the Pungchon limestone host scheelite-rich orebodies including the Sangdong W-Mo deposit (Moon, 1983; Lee, 2001). Pungchon limestone comprises a lower gray limestone, a middle dolomite-rich zone, and an upper milky-white marble (Kim and Lee, 2000), and also hosts numerous W, Fe, and Zn-Pb ore deposits (Yun and Einaudi, 1982; Lee et al., 1990; Moon, 1991b; Koh et al., 1992; Lee et al., 1998; Lee et al., 2007). In its upper part, re-crystallized calcite in high-Ca marble is exploited for high grade calcite (Noh and Oh, 2005; Kim et al.,

Table 1. Stratigraphic column and associated scheelite mineralization in the Taebaeksan metallogenic region (modified as described by Moon, 1989)

Stratigraphy (age)	Formation (thickness in meters)	General lithology	Studied scheelite-bearing samples
Pyeongan Supergroup (Carboniferous–Permian)		Various lithologies incuding shale, sandstone, conglomerate and limestone	
Joseon Supergroup (Cambrian–Ordovician)	Maggol (250–300)	Dark gray limestone and dolomitic limestone	Sinyemi Fe-Zn-Pb (Joongdong area)
	Dumudong (200–250)	Interlayered carbonate-shale, vermicular limestone and sandy shale	Imok Zn-Pb (Joongdong area)
	Dongjeom (20–30)	Dark gray quartzite	
	Hwajeol (100–150)	Interlayered carbonate-shale, vermicular limestone and sandy shale	Sangdong calcite (Sangdong area)
	Pungchon (350–400)	Upper part: milky-white limestone or marble	Sangdong calcite (Sangdong area), Samsung & Seojin calcite (Joongdong area)
		Middle part: light gray dolomitic limestone	Sangdong calcite (Sangdong area)
		Lower part: light gray to dark gray limestone	Sangdong HW W-Mo (Sangdong area)
	Myobong (80–150)	Clay-rich slaty shale with thin carbonate-rich layers or lenses (M1 and F2, F3...)	Sangdong Main-FW W-Mo (Sangdong area)
	Jangsan (150–200)	Light to dark gray quartzite	
Metamorphic basement (Precambrian)		Mica-rich metasedimentary rock (dominantly schist) and granitic gneiss	Sunbawi qtz-scl vein (Sangdong area)

Note: Cc, HW, FW, qtz, and sch represent calcite, Hangingwall, Footwall, quartz, and scheelite, respectively.

https://doi.org/10.1007/s12303-020-0005-z

2017). The Hwajeol and Maggol limestone formations host some Fe-Zn-Pb ore deposits (Kim and Kim, 1978; Kim et al., 1981; Sato et al., 1981; Chang et al., 1990; Kim et al., 2012). The Carboniferous–Permian Pyeongan Supergroup lies unconformably above the Joseon Supergroup. Fluvial sedimentary formations in the late Paleozoic Pyeongan Supergroup host layers of bituminous coal and anthracite (Lee and Lee, 2003).

Joseon Supergroup sedimentary rocks in the Taebaeksan region host numerous magmatic-hydrothermal W-Mo-Fe-Zn-Pb ore deposits, which are associated with late Cretaceous to early Paleogene granitoid intrusions (Hong, 1986; Yun, 1986; Moon, 1987; Chang et al., 1990; Kim and Shin, 1995; Lee et al., 1996b). Scheelite mineralizations include skarns, vein-type mineralization, and carbonate-replacement orebodies occur in the southern part of the Taebaeksan region (Yoo, 2016; Lee et al., 2019). Within the southern part of the Taekbaeksan metallogenic region, orebodies can be further geographically grouped to the Sangdong area in the east and the Joongdong area in the west (Figs. 1 and 2). The Sangdong area hosts the economic Sangdong W-Mo deposit and some nearby subeconomic prospects, whereas the Joongdong area hosts scheelite-bearing sub-economic prospects belonging to Fe-Zn-Pb skarns and high-Ca marble deposits (Sato et al., 1981; Yang, 1991; Choi et al., 2014; Im and Shin, 2016). Sangdong W-Mo deposit is the only economic scheelite deposit in the Taebaeksan region of W production record (Lee, 2001). Other scheelite-bearing prospects have no record of W production, and they contain only trace amount of scheelite and wolframite based on explorations (Moon, 1987; Chi, 2011; Gliddon et al., 2012; Yoon et al., 2013; Wheeler, 2016; Yoo, 2016) and mineralogical studies (Kim et al., 1981; Sato et al., 1981; Yang, 1991; Seo et al., 2007; Choi et al., 2014; Im and Shin, 2016).

2.2. Mineralization in The Sangdong Area: The Sangdong W-Mo Deposit and Unmineralized Prospects

In the Sangdong area, we studied scheelite in the economic Sangdong W-Mo deposit, unmineralized skarns within Sangdong calcite mine, and unmineralized Sunbawi quartz-scheelite veins

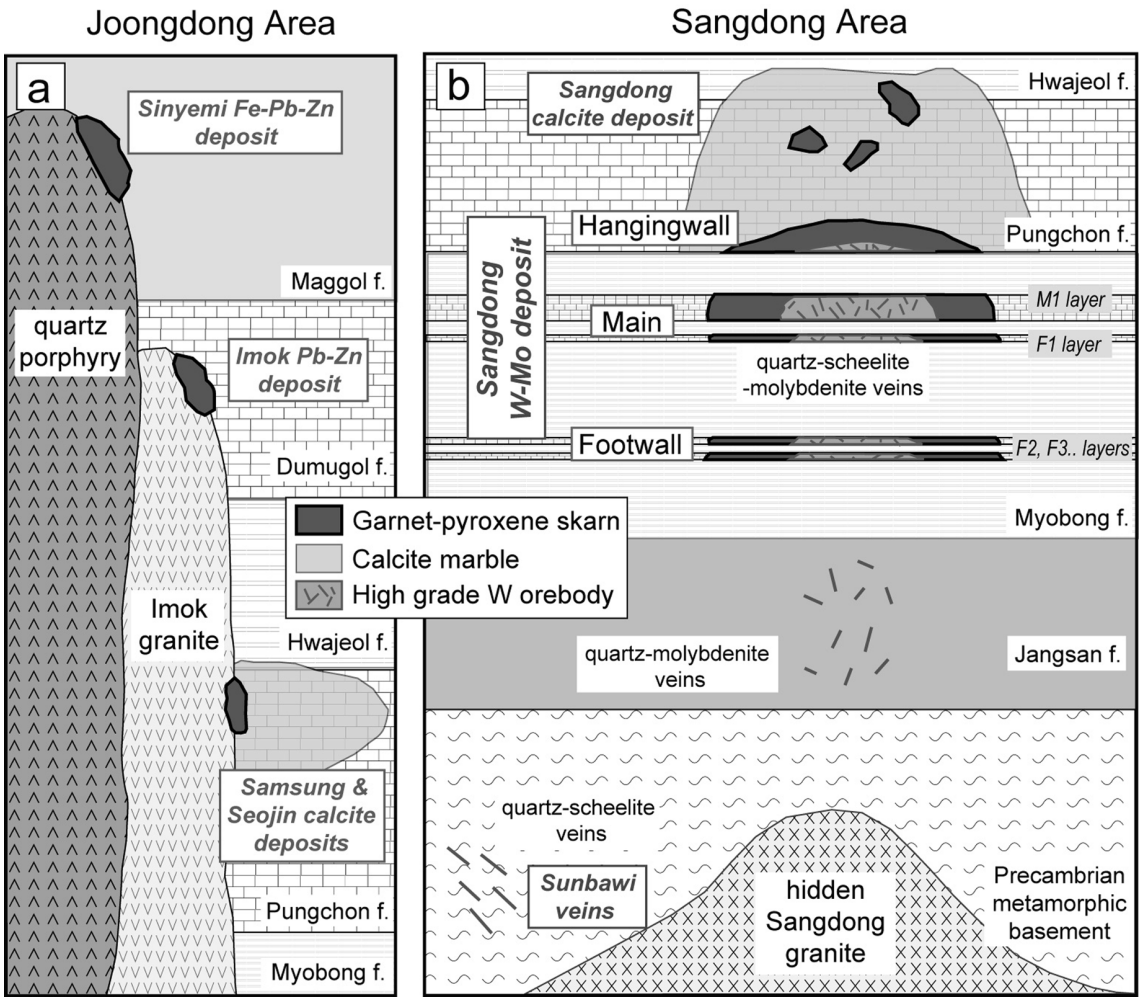

Fig. 2. Schematic illustration showing stratigraphy, granitoid intrusions, and associated scheelite mineralization in the Joongdong (a) and Sangdong (b) areas. Lithology details of each formation and stratigraphic unit can be found in Appendix 1 (Table S1).

(Fig. 2). The Sangdong deposit is a stratabound W-Mo ore deposit hosted in the carbonate-rich layers of the Myobong formation and in the lower part of the Pungchon formation. The thickest carbonate-rich layers (M1 and F1 layers are around 6 and 2 m thick, respectively) of the Myobong formation host major W-Mo mineralization and constitute the Main orebody. Thinner carbonate-rich layers beneath the M1 and F1 layers (the F2, F3... layers, which are 0.3–7 m thick) host the Footwall orebody. The lowermost part of the Pungchon formation hosts the Hangingwall orebody (Moon, 1984a, 1984b, 1985, 1986). All orebodies in the Sangdong deposit consist of early skarns with an anhydrous mineral assemblage including wollastonite-garnet-pyroxene followed by two stages of hydrothermal quartz veins (Figs. 3 and 4), which are characterized by amphibole alteration and biotite-muscovite alteration, respectively (Seo et al., 2017). Early skarn hosts a minor amount of disseminated scheelite (0.1–0.3 wt% WO_3). In the vein stages, early quartz veins are associated with amphibole-quartz alteration host magnetite, pyrrhotite, and minor disseminated scheelite (0.3–1.0 wt% WO_3), whereas later quartz veins are associated with biotite-muscovite-quartz alteration, host coarse-grained scheelite, and molybdenite (1.0–3.0 wt% WO_3) (Lee, 2001). Some quartz veins associated with biotite-muscovite-quartz alteration are crosscut by sub-parallel quartz-fluorite veins with muscovite-quartz alteration, and these latter veins host carbonate minerals and sulfides including chalcopyrite, sphalerite, and galena. For detailed descriptions of this deposit refer to Seo et al. (2017) and the references therein. The age of mineralization in the Sangodng W-Mo deposit is ~87 Ma, based on Ar-Ar dating of muscovite (Seo et al., 2017), and the depth of the Main orebody estimated by fluid inclusion microthermometry is about 1–3 km below the paleosurface (Seo et al., 2017).

Although igneous rocks are not exposed near the Sangdong deposit, drilling surveys found a hidden granite (Sangdong granite: Figs. 2 and 3) that is a magnetite series muscovite-bearing equigranular

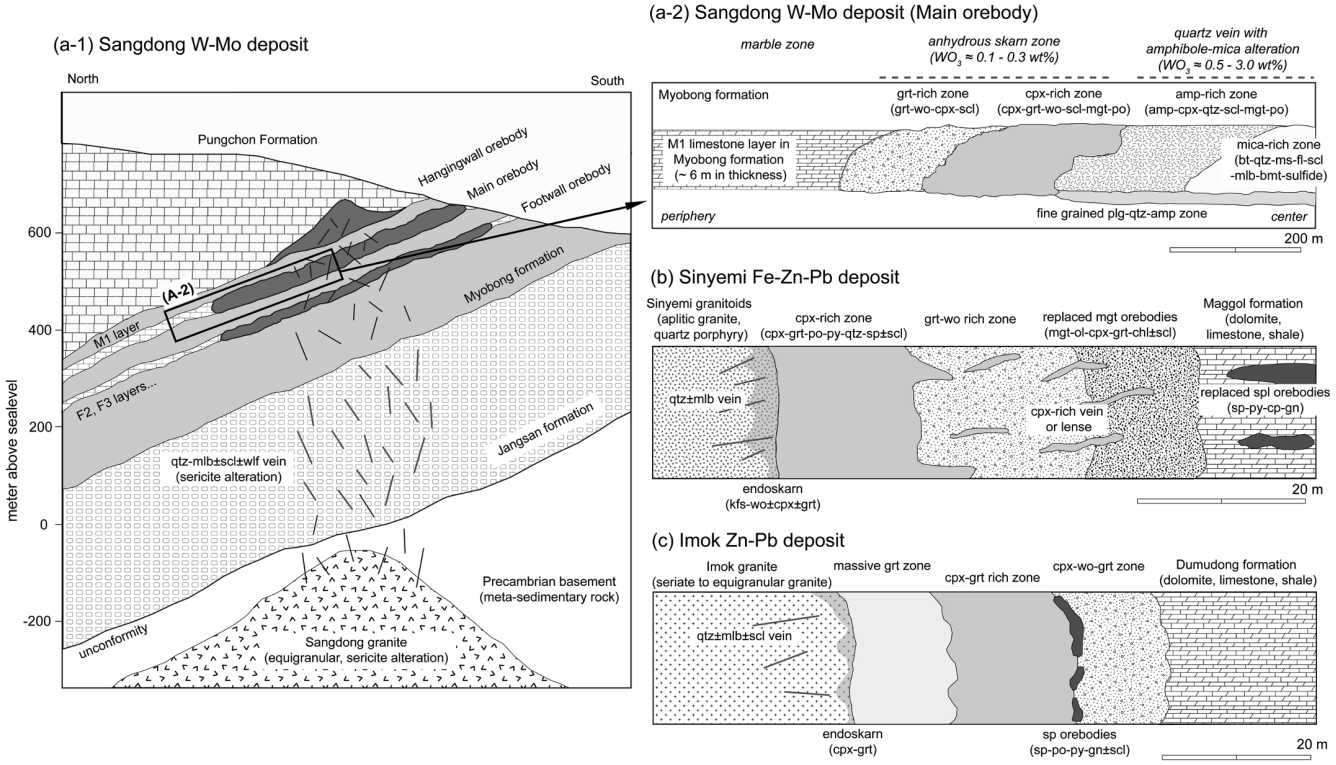

Fig. 3. Illustrations of skarn zonation, association of igneous intrusions, and occurrence of scheelite in Sangdong W-Mo (a-1 and a-2), Imok Zn-Pb (b), and Sinyemi Fe-Zn-Pb (c) deposits in Taebaeksan metallogenic region (Moon, 1983; Yang, 1991; Seo et al., 2007; Im and Shin, 2016; Seo et al., 2017). Zones of exoskarn minerals in the Sinyemi (about 50–100 m) and the Imok deposits (about 40–80 m) are closely associated and spatially contact with igneous intrusions, and the intrusions host both endoskarns and quartz veins bearing minor molybdenite or scheelite. While much larger zoned exoskarns are formed in the Sangdong deposit (about 1 km to 2 km), no igneous intrusions are exist on the surface. Sangdong granite about 700–900 m below the Main orebody were located by drill hole survey (Lee, 2001). The Sangdong granite have sericite alteration and trace amount of sulfide minerals including molybdenite (Kim, 1986; Moon, 1987). Quartz veins with molybdenite or scheelite or wolframite mineralization are hosted in rocks in between the Sangdong granite and the Sangdong W-Mo orebodies. The quartz veins associate sericite or biotite-muscovite alteration. The magmatic-hydrothermal fluids from the Sangdong granite might be channelized by the major strike–slip faults in the Sangdong area and might be causative for the Sangdong W-Mo mineralization (Moon, 1987; Kim and Shin, 1995; Seo et al., 2017). Abbreviations: qtz = quartz, mlb = molybdenite, amp = amphibole, pl = plagioclase, grt = garnet, sp = sphalerite, py = pyrite, ms = muscovite, gn = galena, cp = chalcopyrite, scl = scheelite, ol = olivine, po = pyrrhotite, wo = wollastonite, mgt = magnetite, bmt = bismuthinite, wlf = wolframite, fl = fluorite, bt = biotite, sulfide = base metal sulfides, kfs = k-feldspar, chl = chlorite, and cpx = clinopyroxene.

https://doi.org/10.1007/s12303-020-0005-z

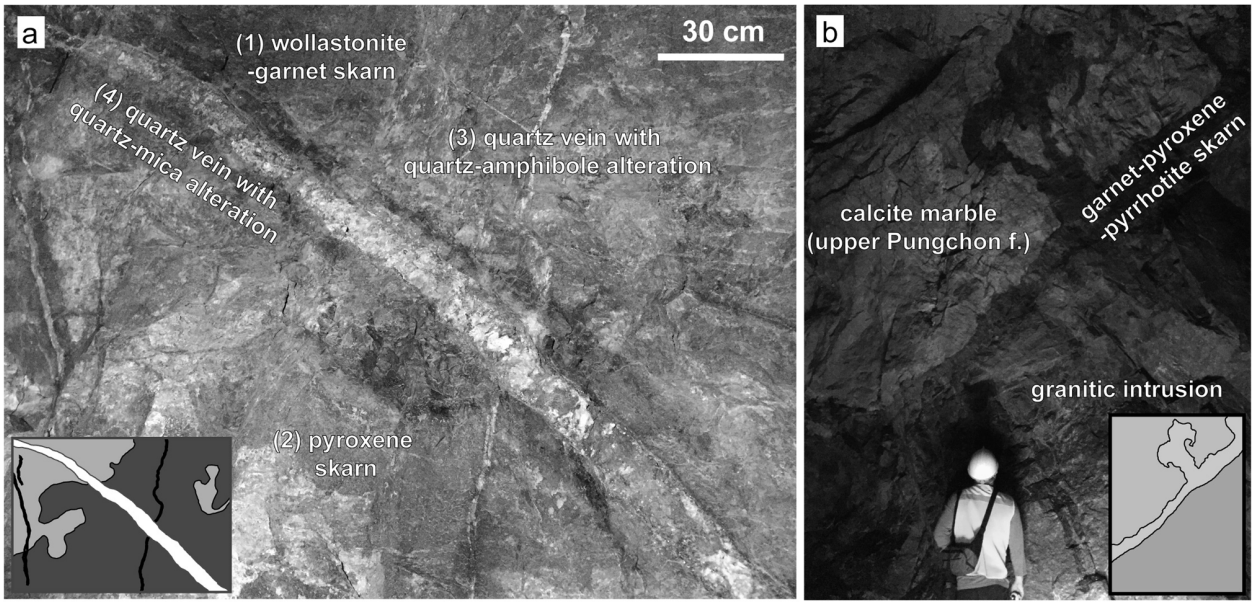

Fig. 4. Photographs of underground outcrops showing overprinting and crosscutting relationships in scheelite-bearing orebodies. (a) Main orebody in the Sangdong W-Mo deposit showing spatial and temporal relationships of (1) wollastonite skarn, (2) pyroxene skarn, (3) quartz-amphibole-scheelite veins, and (4) the quartz-mica-scheelite-molybdenite vein. (b) Intrusive contact of Imok granite with calcite marble in the Seojin calcite deposit in the Joongdong area. A thin garnet-pyroxene skarn contains disseminated subeconomic scheelite.

monzogranite dated at 87.5 Ma (Go, 1986; Kim, 1986; Moon, 1987; Moon, 1989; Kim and Shin, 1995). The occurrence of Sangdong granite from a drill hole indicated the granite has the shape of a sharp apophysis or cupola of greater batholithic magma (Kim, 1986; Moon, 1987), and its mineralogy and trace element chemistry suggested the granite was fluid saturated and might correspond to the latest stage of fractionation among the Cretaceous granitoids intruded in the Korean peninsula (Moon, 1987). Sr and Nd isotopes indicated the Sangdong granite is mantle-derived with a significant crustal contribution (Kim and Shin, 1995). Concentrations and normalized patterns of REE in Sangdong granite and skarns were similar, although their Eu anomaly values differed (Moon, 1989), which suggests the skarn was derived from a granitic source, and that in REE patterns were modified by its mineral assemblage (Moon, 1989). The orebodies in the Sangdong W-Mo deposits are situated between two major N-S trending sub-vertical clockwise strike-slip faults (Fig. 5a), namely, the Guraeri (N5E, vertical) and Mingol (N5E, 5SE) faults. Numerous minor faults constitute fracture zones between these two major faults, and may have provided a channel for ore-forming magmatic-hydrothermal fluids responsible for W-Mo ore formation. We collected scheelite-bearing samples from the Main, Footwall, and Hangingwall orebodies from different stages of mineralization and included samples from early skarn and later quartz veins. These scheelite-bearing samples were collected from outcrops in underground mines and drill cores.

Adjacent to the Sangdong W-Mo deposit is a re-crystallized high-Ca calcite marble deposit, the Sangdong calcite mine (Figs. 1 and 2). This calcite deposit is located in the upper Pungchon and Hwajeol limestone formations, stratigraphically directly above the W-Mo orebodies. In the Sangdong calcite mine, minor local occurrences of pyroxene-magnetite-pyrrhotite skarns with disseminated scheelite occur between the two major strike-slip faults (Fig. 5a). Scheelite in the calcite mine is often disseminated or associated with quartz-fluorite veins. We collected scheelite-bearing skarn samples from an outcrop underground, and sampled the quartz-fluorite-scheelite vein from drill cores.

The Sunbawi quartz-scheelite veins are located SW of the Sangdong W-Mo deposit and are hosted in Precambrian mica-rich meta-sandstones (Figs. 1 and 2). In these veins, sub-economic concentrations of scheelite are hosted within sub-parallel (strike direction about EW and dip direction 60–70N) 1–5 cm thick quartz-pyrite veinlets with muscovite-quartz alteration selvages. These selvages are dated at 87–89 Ma, based on Ar-Ar ages of muscovite, that is, they are of around the same age as the Sangdong W-Mo deposit (Seo et al., 2017). Several undocumented exploration adits exist in the Sunbawi area (Moon, 1987; Yoon et al., 2013), and we also collected samples from quartz-scheelite veins in these adits.

2.3. Scheelite-bearing Subeconomic Prospects in The Joongdong Area

The Sinyemi deposit in the Joongdong area consists of skarn and carbonate-replacement type orebodies (Fig. 3) and is hosted in the Maggol limestone of the Joseon Supergroup. The deposit

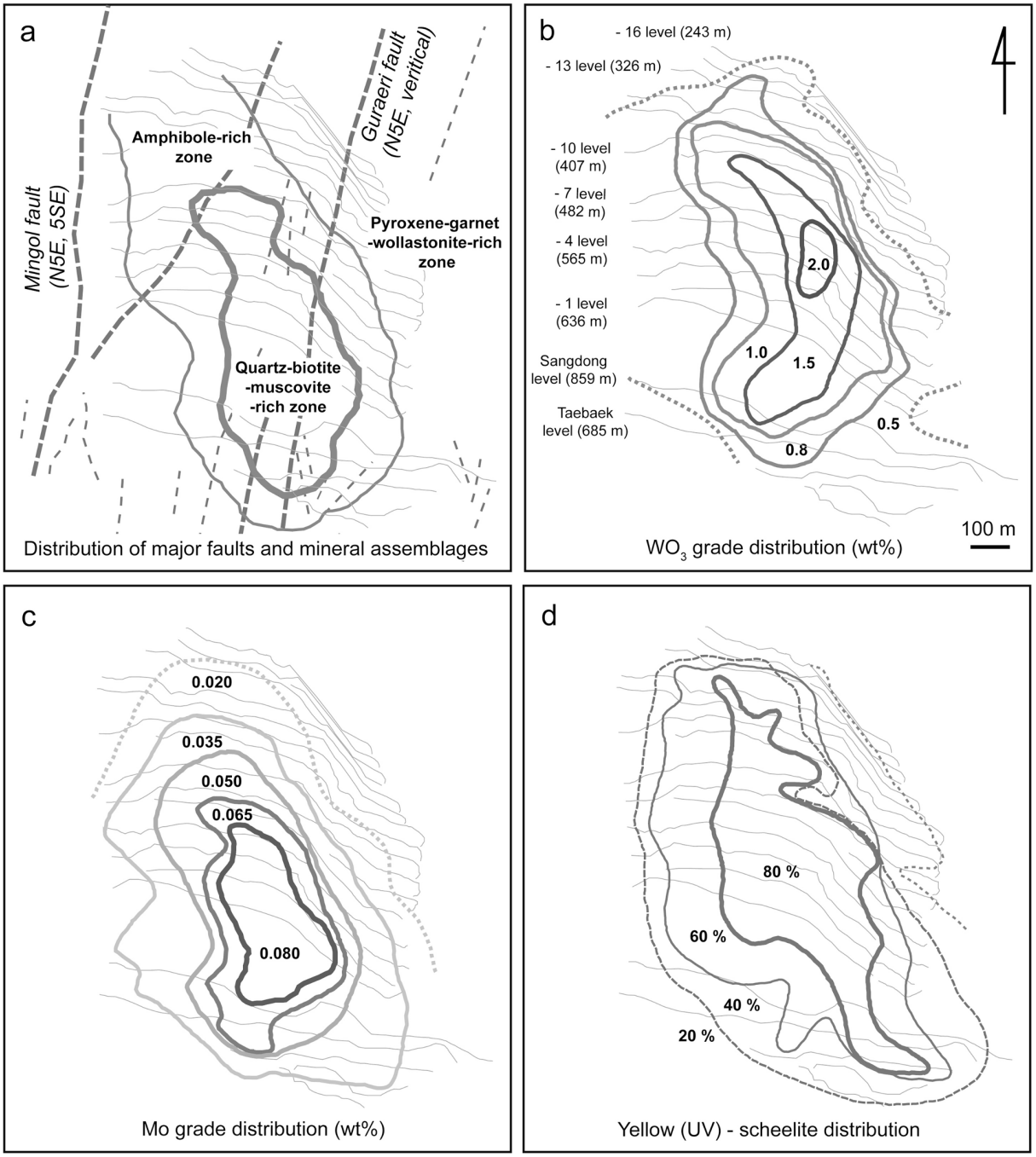

Fig. 5. The overview of the mine-scale distribution of major and minor strike-slip faults (dextral) and zonations of skarn and alteration minerals (a), ore grade WO_3 (b) and Mo (c), and yellow fluorescent scheelite (d) in the Sangdong W-Mo deposit. The gray lines with brackets represent levels of underground mining and elevations (above sea level). North-south striking faults including the Mingol and Guraeri faults are dominant around the deposit. High-grade W-Mo mineralization in the center of the deposit with mineralogy of quartz-biotite-muscovite contains more yellow fluorescent scheelite than the low-grade periphery. Modified as described by Moon (1983), Go (1986), and Lee (2001).

consist of two orebodies, a Fe-Zn ± Mo skarn and a carbonate-replacement Zn-Pb deposit; both are closely associated with Cretaceous Sinyemi granitoid intrusions of aplitic granite and quartz porphyry (Kim and Kim, 1978; Kim et al., 1981; Sato et al., 1981; Kim and Nakai, 1982; Choi et al., 2014). Phlogopite K-Ar ages of the orebodies are 75 to 78 Ma (Sato et al., 1981; Park et al., 1988). This deposit has produced about 2.8 Mt of Fe and Zn, Cu, Mo, and Pb as by-products (Choi et al., 2009). We collected drill core samples of disseminated scheelite in the magnetite-calcite bearing skarn.

The Imok Zn-Pb deposit in the Joongdong area is a combined skarn, carbonate-replacement, vein type deposit. It is hosted in the Dumudong calcareous shale of the Joseon Supergroup (Fig. 3). This deposit exhibits close spatial association with coarse-

https://doi.org/10.1007/s12303-020-0005-z

grained Cretaceous Imok granitoids. Early pyrrhotite-bearing garnet-pyroxene skarn mineralization with sub-economic disseminated scheelite is crosscut by pyrrhotite-sphalerite-galena veins. The clay K-Ar age of mineralization is between 83 and 97 Ma (Im and Shin, 2016). We collected a scheelite-bearing pyrrhotite skarn sample from an underground outcrop.

At two neighboring mines, the Seojin and Samsung calcite deposits, high-Ca marble is exploited from the upper part of the Pungchon limestone formation (Figs. 1 and 2). Both deposits are spatially associated with the Imok granitoid. Small-scale pyroxene-pyrrhotite bearing skarns occur around a contact zone in the limestone (Fig. 4b). We collected samples of disseminated scheelite from the pyrrhotite-rich zone from an underground outcrop and drill cores.

3. PETROGRAPHY OF SCHEELITE-BEARING SAMPLES

Detailed petrographic information including details of mineral assemblage and a description of the alteration features of the scheelite samples studied are provided in Appendix 1 (Electronic supplementary material, Table S1). Scheelite is generally fine-grained and disseminated in the wallrock matrix (e.g., skarn or altered rock), while veins host both coarse- and fine-grained scheelite. Scheelite from the Taebaeksan region shows a range of fluorescence colors from blue to yellow under a short-wavelength UV light. We classified scheelite based on fluorescence color into four types: blue, blue-white, white, and yellow (Fig. 6). Most of the fine-grained scheelite crystals had relatively uniform fluorescence colors, whereas coarse-grained scheelite often had various fluorescence colors, although it was difficult to macroscopically distinguish zonation patterns.

3.1. Scheelite in The Sangdong W-Mo Deposit

Scheelite occurs in several ore-bearing stages within the Sangdong W-Mo deposit. Early skarn-stage scheelite is fine-grained and generally disseminated in a matrix of pyroxene, pyrrhotite, and magnetite. Scheelite in quartz veins associated with amphibole-quartz alteration is generally fine-grained and disseminated

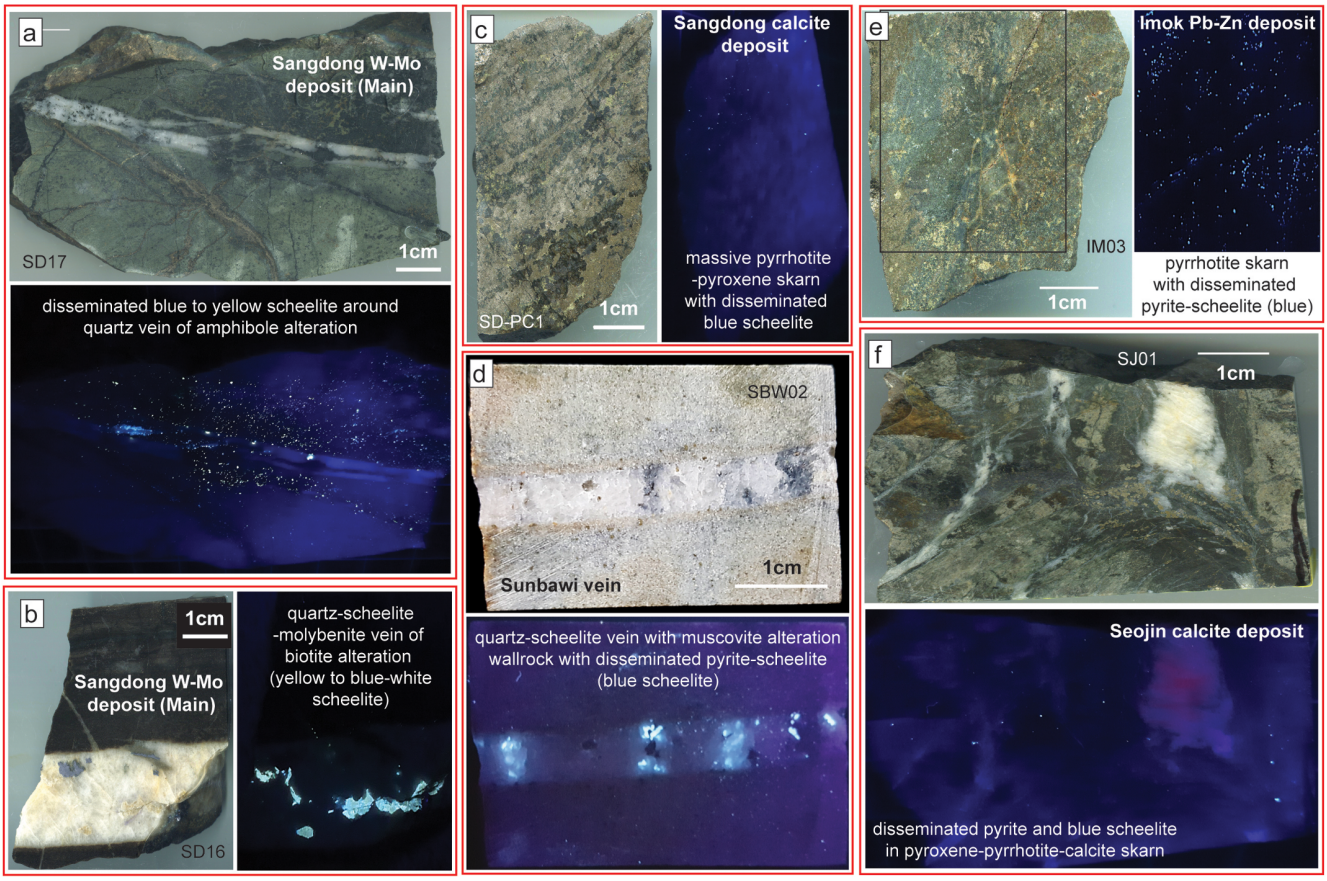

Fig. 6. Scheelite-bearing ores and fluorescence features under short-wavelength UV light in the Main orebody in the Sangdong W-Mo deposit (mixture of yellow and blue scheelite in a and b), pyroxene-pyrrhotite skarn in the Sangdong calcite marble deposit (c), quartz-scheelite vein with muscovite alteration in the Sunbawi area (d), pyroxene-pyrrhotite skarn in the Imok deposit (e) and pyroxene-pyrrhotite-calcite skarn in the Seojin calcite deposit (f). Note that some scheelite in samples from the Sangdong W-Mo deposit (a and b) fluoresced yellow, whereas scheelites from unmineralized locations (c–f) fluoresced blue or blue-white.

within the alteration selvage of wallrock and within quartz veins (Fig. 6a), whereas scheelite in the later quartz-scheelite-molybdenite vein associated with biotite-muscovite-quartz alteration was generally coarse-grained (Fig. 6b). In some of the latter quartz veins, scheelite replaced early wolframite and was closely associated with coarse-grained molybdenite. Late-stage quartz-fluorite veins with muscovite-quartz alteration halos crosscut earlier veins and the skarn matrix. Open vugs in the centers of late-stage veins were filled with sulfide and carbonate minerals with only minor scheelite. Rutile is present in all scheelite-bearing quartz veins in the Sangdong deposit (Seo et al., 2017) and typically occurs at vein and altered wallrock contacts. Scheelite in the Sangdong deposit fluoresces yellow, white, blue-white, and blue. At the center of the Sangdong deposit, yellow fluorescing scheelite is most common, whereas blue scheelite is more common in the low-grade periphery (Fig. 5a).

3.2. Scheelite in Subeconomic Prospects of The Sangdong Area

In the Sunbawi quartz vein, coarse-grained scheelite is associated with pyrite and minor molybdenite. Quartz veins are associated with muscovite-quartz alteration, and disseminated scheelite occurs in altered wallrock. Scheelite from the Sunbawi vein typically fluoresces blue (Fig. 6d). In the Sangdong calcite deposit, scheelite in the pyrrhotite-rich pyroxene skarn is disseminated and fine-grained, and hosted in the re-crystallized calcite marble of the upper Pungchon limestone formation. In the Hwajeol limestone formation, disseminated and fine-grained scheelite occurs within interstitial fluorite of garnet-pyroxene skarn or in skarn matrix. Scheelite in the Sangdong calcite deposit typically fluoresces blue, but blue-white and white types are also observed (Fig. 6c).

3.3. Scheelite in Subeconomic Prospects of The Joongdong Area

In the Sinyemi Fe-Zn-Pb deposit, fine-grained scheelite is disseminated in calcite-epidote-pyroxene skarn. Magnetite and sphalerite are also present in skarn matrix. Scheelite in the Sinyemi sample are dominantly fluoresces blue. Disseminated pyrite and minor scheelite occur in the pyrrhotite-rich pyroxene skarn in the Imok Zn-Pb deposit, and these scheelite crystals typically fluoresce blue (Fig. 6e). In the Seojin and Samsung calcite deposits, fine-grained scheelite is disseminated in the pyrrhotite- and magnetite-rich garnet-pyroxene skarn in re-crystallized marble and fluoresces blue-white and blue (Fig. 6f).

4. LA-ICP-MS MICROANALYSIS

Scheelite grains (n = 64) were studied in 25 samples from 10 orebodies in the southern Taebaeksan region. Following petrographic analysis, scheelite samples were mounted as polished, ~100 μm thick sections. Alteration relationships, mineral assemblages, and the fluorescence colors of scheelite crystals were examined (Appendix 1 (Table S1)), prior to LA-ICP-MS (laser ablation inductively coupled plasma mass spectrometry) microanalysis, which was conducted at ETH Zurich and the Korea Polar Research Institute (KOPRI), which both have 193 nm ArF Excimer laser ablation systems connected to a quadruple ICP-MS (Perkin Elmer Elan 6100 DRC at ETH and i Cap-Q model at KOPRI). A dwell

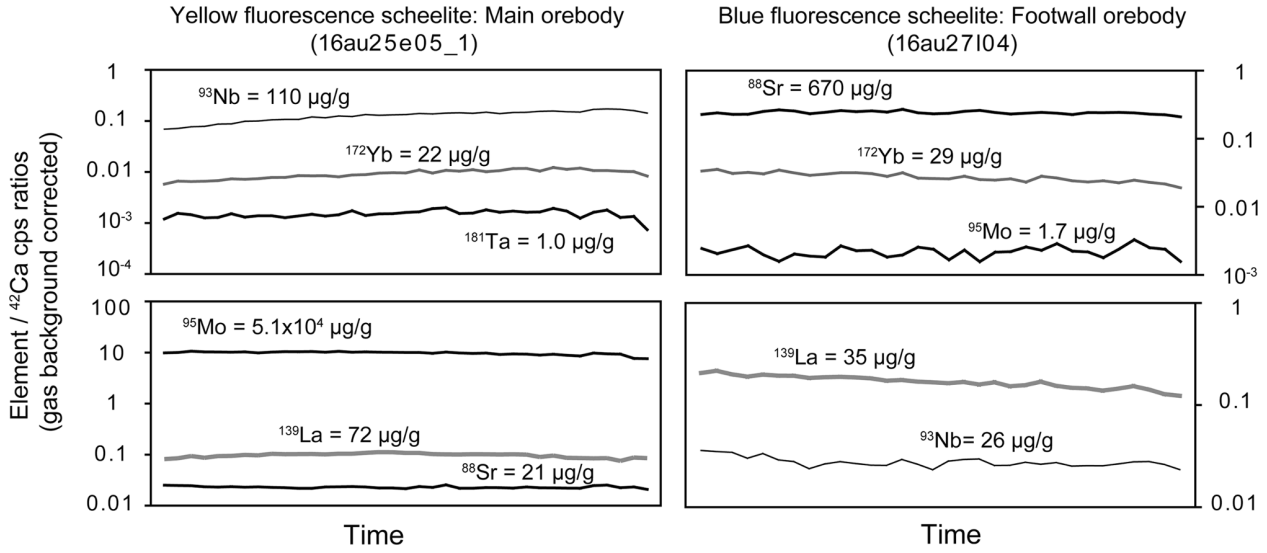

Fig. 7. Time-resolved transient signals obtained by LA-ICP-MS analysis of scheelite grains. Counts per second (cps) ratios of some representative trace elements (Nb, Yb, Ta, Mo, La, and Sr) normalized versus Ca after gas background correction. Trace element cps ratios in scheelite were flat and stable for very low (1.7 μg/g) and very high (5.1 wt%) Mo concentrations, indicating elements were incorporated as substituting cations in the scheelite structure.

https://doi.org/10.1007/s12303-020-0005-z

time of 10 ms was used for each isotope analyzed, that is, for ^{7}Li, ^{11}B, ^{23}Na, ^{42}Ca, ^{55}Mn, ^{57}Fe, ^{69}Ga, ^{72}Ge, ^{75}As, ^{85}Rb, ^{88}Sr, ^{89}Y, ^{93}Nb, ^{95}Mo, ^{139}La, ^{140}Ce, ^{141}Pr, ^{146}Nd, ^{147}Sm, ^{151}Eu, ^{157}Gd, ^{159}Tb, ^{163}Dy, ^{165}Ho, ^{166}Er, ^{169}Tm, ^{172}Yb, ^{175}Lu, ^{181}Ta, ^{182}W, ^{208}Pb, ^{209}Bi, ^{232}Th, and ^{238}U. The beam diameter of the laser was varied from 25 to 150 μm depending scheelite crystal size, to optimize the detection of trace elements. Energy densities on mineral surfaces were between 20–30 J/cm^2. Frequencies of pulses were adjusted from 2 to 10 Hz to control LA-ICP-MS transient signals to allow consistent trace element detection. Trace element concentrations were obtained using SILLS software (Guillong et al., 2008) and NIST 610 glass as an external standard and stoichiometric Ca concentrations in scheelite (13.9 wt% Ca) as an internal standard. As part of the data reduction scheme, elemental ratios were monitored (Fig. 7) to allow time-resolved anomalies in spectra (e.g., inclusions) to be eliminated from the analysis.

5. RESULTS

Scheelite in the Taebaeksan region routinely contains detectable concentrations of Nb, Mo, Sr, and REE by LA-ICP-MS microanalysis; Ta, Hf, Cs, Na, Ba and Rb were observed at only just above detection limits in some scheelite samples. Concentrations of the trace elements determined in scheelite and information including alteration features and fluorescence colors are provided in the Appendices 2 and 3 (Electronic supplementary material, Tables S2 and S3).

Chondrite-normalized REE patterns in scheelites showed negative to positive Eu anomaly values and flat to slightly middle REE enriched patterns (Fig. 8). Significant Nb/Ta ratio and Nb scheelite concentration differences were observed between the Sangdong W-Mo deposit and other scheelite-bearing prospects (Figs. 9 and 10). Scheelite from the Sangdong W-Mo deposit showed a negative correlation between Nb concentration and Eu anomaly values ($y = -22.9x + 103.1$, $R^2 = 0.13$; Fig. 9) and a positive correlation between Nb and total REE concentration ($y = 4.6x + 446.5$, $R^2 = 0.37$; Fig. 11b). Sr concentrations were highly variable throughout the region (Fig. 12). Ce anomaly values in scheelite were obvious (Fig. 8), and negative correlations were observed between Mo and Sr concentrations in the Sangdong W-Mo deposit (Fig. 13b).

5.1. Scheelite Composition in The Sangdong W-Mo Deposit

Scheelite in the Sangdong W-Mo deposit had highly variable

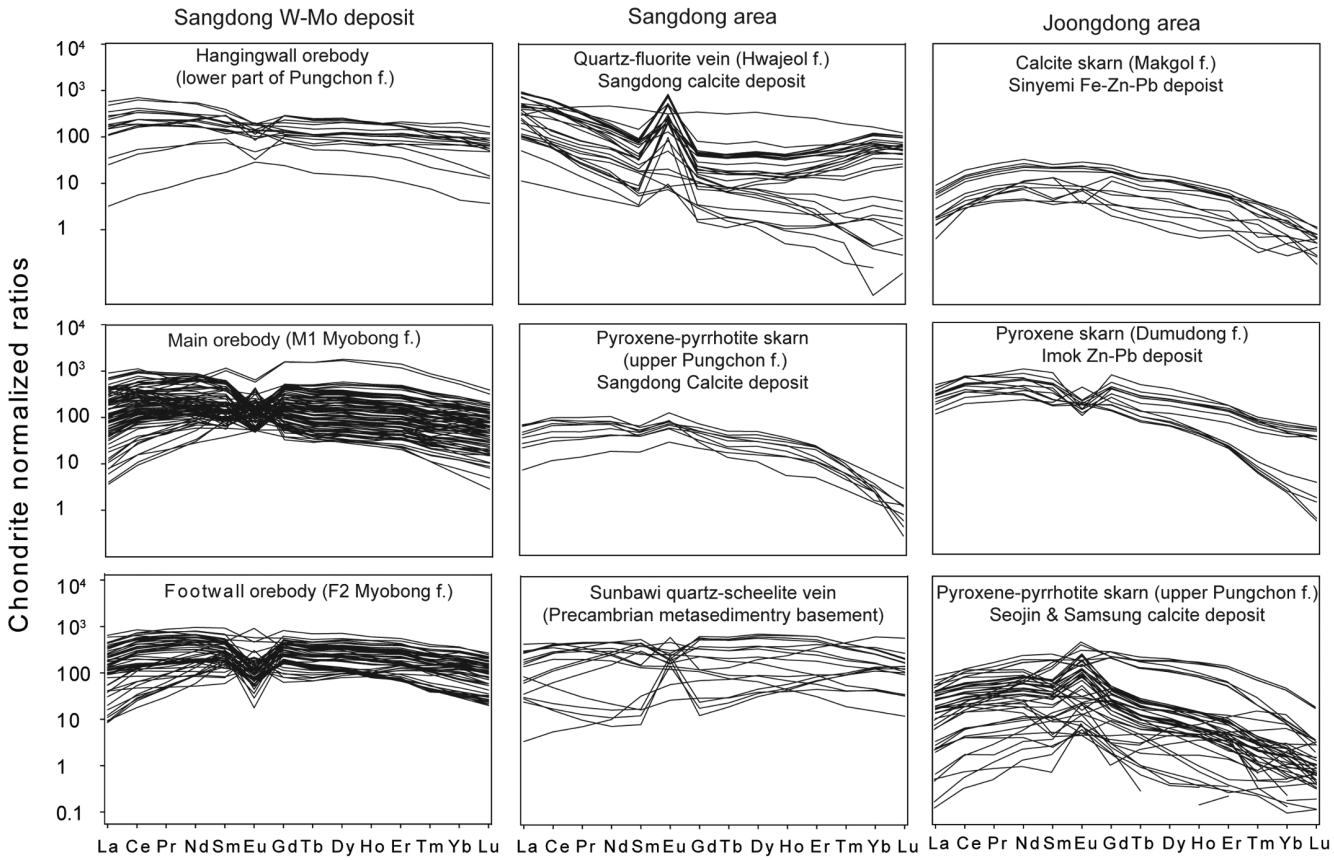

Fig. 8. Chondrite-normalized REE pattern of orebodies in the Taebaeksan metallogenic region. Various degrees of Eu and Ce anomaly values were obvious in orebodies of the Sangdong W-Mo deposit.

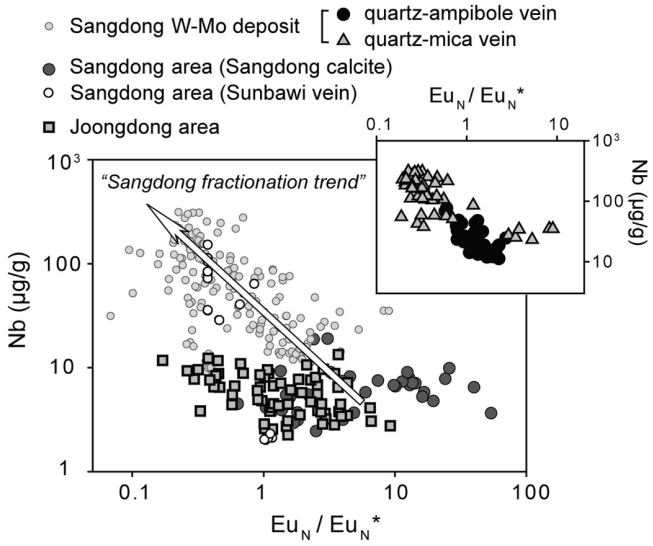

Fig. 9. Plot of Nb versus Eu anomaly values ($Eu_N/*Eu_N$) for scheelite from the southern Taebaeksan region. A broadly negative trend of Nb versus Eu anomaly values of a speculative "Sangdong fractionation trend" is obvious. Scheelite from the Joongdong area contained less Nb than the Sangdong W-Mo deposit. In the Sangdong deposit, scheelite associated with quartz-amphibole veins had lower Nb concentrations and higher Eu anomaly values than scheelite in texturally later quartz-mica veins. Some scheelite in Sunbawi veins in the Sangdong area closely overlapped with the Sangdong W-Mo deposit. Data from the Sangdong granite are from Moon (1989).

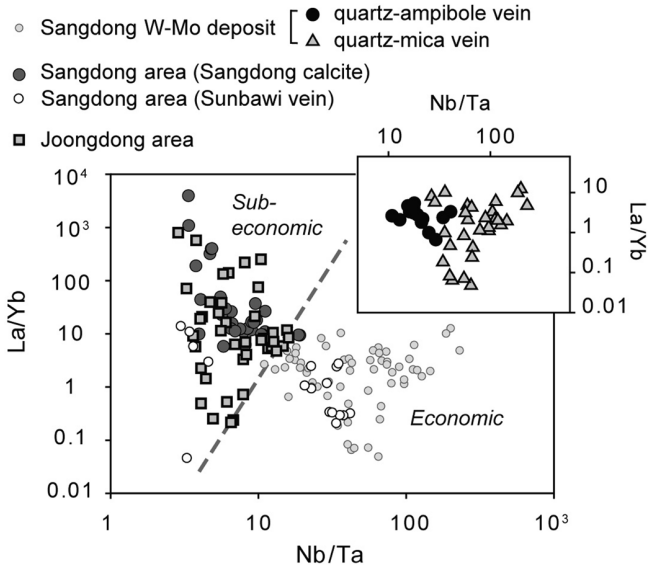

Fig. 10. Plot of Nb/Ta versus La/Yb ratios in scheelite from the southern Taebaeksan region. Scheelites from the economic Sangdong W-Mo deposit were discriminated from scheelite in subeconomic occurrences, except for some scheelites from the Sunbawi vein in the Sangdong area.

Nb and Sr concentrations (from 7 to 310 μg/g (average: 82 μg/g) and from 13 to 710 μg/g (average: 78 μg/g), respectively). The Mo content of scheelite displayed an even greater range from 0.1 to 51,000 μg/g (average: 78 μg/g). Flat cps ratio curves in LA-ICP-MS transient signals during ablation of scheelite from the

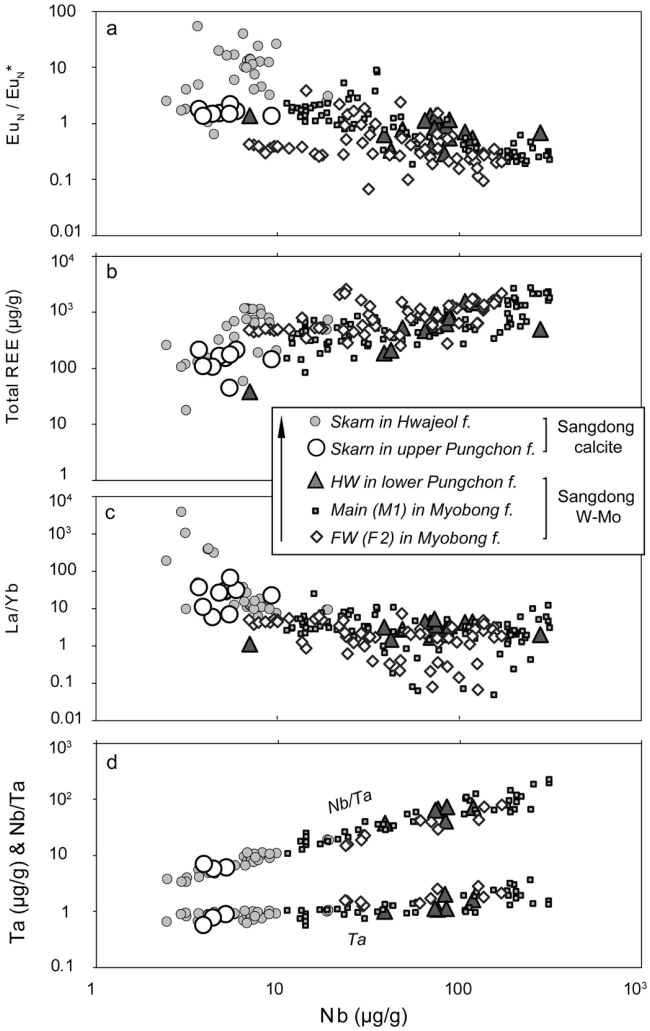

Fig. 11. Nb concentrations versus (a) Eu anomaly values, (b) total REE concentrations, (c) La/Yb ratios, and (d) Ta concentrations and Nb/Ta ratios for scheelite from the Sangdong W-Mo and Sangdong calcite deposits showing stratigraphic relationships of scheelite-bearing orebodies in the Sangdong area. The arrow indicates scheelite hosted in the upper sedimentary unit. Relatively lower total REE concentrations, lower Ta concentrations, higher La/Yb ratios, and higher Eu anomaly values in the Sangdong calcite deposit suggest lower fractionation degrees from causative magma. Higher Nb/Ta ratios in the Sangdong W-Mo deposit might be explained by a hydrothermal rutile precipitation concomitant to scheelite precipitation.

Main orebody (Fig. 7) indicated that the high Mo concentration of ~5 wt% was due to substitution in the lattice. Total REE concentrations were 39–2,800 μg/g (average: 830 μg/g) and Nb/Ta ratios ranged from 11 to 230 (average: 59). Nb/Ta ratios in the Hangingwall, Main, and Footwall orebodies had closely overlapping ranges of 38–74, 11–230, and 15–80, respectively. In the Main orebody, scheelite from quartz veins associated with amphibole-quartz alteration had total REE concentrations of 83–790 μg/g (average: 380 μg/g) and Nb/Ta ratios of 11–41 (average: 21), while scheelite from quartz veins associated with biotite-muscovite-quartz alteration had higher total REE concentrations of 270–

https://doi.org/10.1007/s12303-020-0005-z

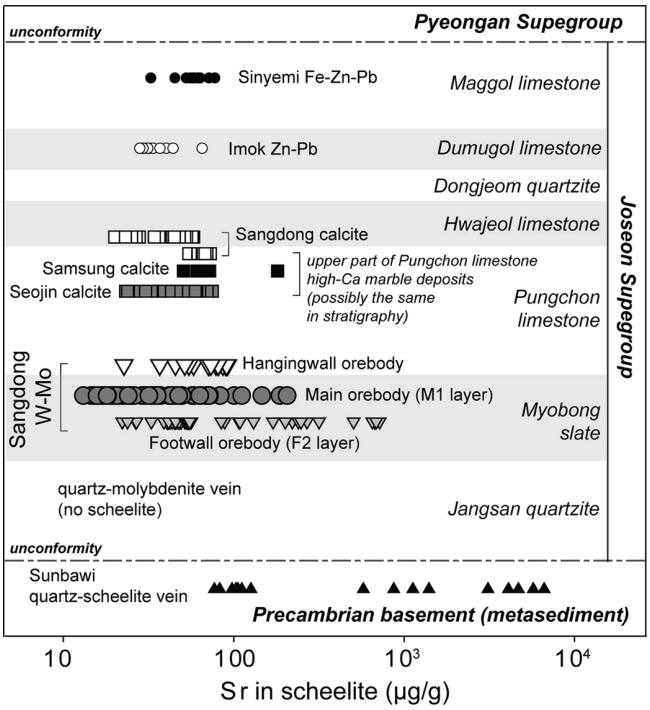

Fig. 12. Range of Sr concentrations in scheelite in orebodies hosted in various stratigraphic units in the Taebaeksan region. With the exception of the Sunbawi vein hosted in metamorphic basement which exhibited the largest range, scheelite in the Sangdong W-Mo deposit exhibited a larger Sr concentration range than other subeconomic prospects hosted in the Paleozoic sedimentary units in the Joseon Supergroup. In the Sangdong W-Mo deposit, scheelite associated with quartz vein of biotite-muscovite-quartz alteration had a larger Sr concentration range than scheelite in the quartz vein with amphibole alteration.

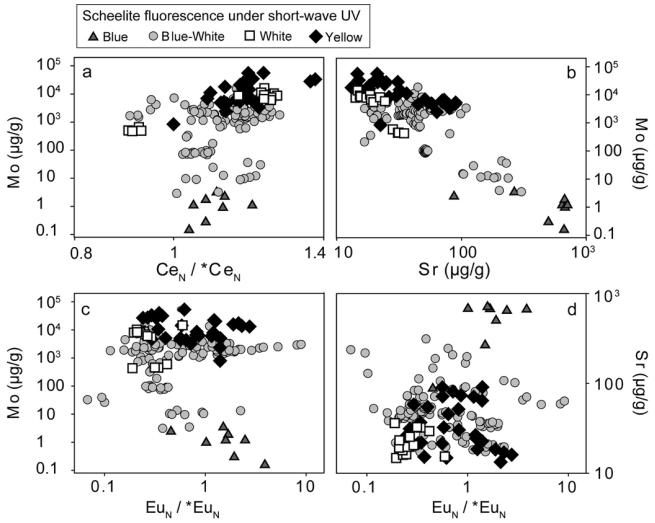

Fig. 13. Mo, Sr concentrations, Eu ($Eu_N/*Eu_N$), and Ce anomaly values ($Ce_N/*Ce_N$) for scheelite in the Sangdong W-Mo deposit and its fluorescence colors under short-wavelength UV light. Yellow fluorescing scheelite had the highest and blue scheelite have the lowest Mo concentration (a–c). Sr and Mo concentrations were negatively correlated (b). Some of the yellow scheelite had the largest Ce anomaly value (a). Eu anomaly values were not correlated with Sr or Mo concentrations (c and d).

2,800 μg/g (average: 1,100 μg/g) and Nb/Ta ratios of 26–230 (average: 84). In the Main orebody, Sr concentrations in scheelite from the biotite-muscovite-quartz alteration stage ranged from 15–209 μg/g (average: 51 μg/g) and were much larger than in the amphibole-quartz alteration stage (13–64 μg/g; average: 29 μg/g). Maximum Mo concentrations in blue, blue-white, and yellow fluorescing scheelite were 3, 17,000, and 51,000 μg/g, respectively.

REE values of scheelite normalized to chondrite (Anders and Grevesse, 1989) showed a wide spectrum of Eu anomaly values (Figs. 7 and 9) in the Sangdong W-Mo deposit. Eu anomaly values calculated using Eu_N/Eu_N^* (Eu_N^* = average of normalized Sm and Gd values) ranged from 0.07 to 9.00, and were negatively correlated with Nb concentrations in Sangdong W-Mo deposit scheelite. Eu anomaly values and Nb concentrations of the hidden Sangdong granite (Moon, 1984a, 1989) are ploted slightly lower but within the trend of the Sangdong scheelite (Fig. 9). Total REE concentrations and La/Yb ratios also showed correlations with Nb and Nb/Ta, respectively (Figs. 10 and 11). Ce anomaly values calculated using Ce_N/Ce_N^* (Ce_N^* = average of normalized Sm and Gd values) ranged from 0.90 to 1.37, and maximum Ce anomaly value in scheelite had the highest Mo concertation and fluoresced yellow (Fig. 13a). Mo and Sr concentrations in scheelite were strongly associated with fluorescence colors from blue to yellow (Fig. 13b).

5.2. Subeconomic Prospects in The Sangdong Area

Scheelites from the Sunbawi quartz vein hosted in Precambrian metamorphic rocks had Nb concentrations and Nb/Ta ratios of 2–150 μg/g (average: 57 μg/g) and of 3–41 (average: 23), respectively, which overlapped with those of the Sangdong W-Mo deposit (Figs. 9 and 10). Sr concentrations exhibited a relatively wide range from 77 to 6,600 μg/g (average: 1,700 μg/g), Eu anomaly values ranged from 0.37 to 19.66, and total REE concentrations from 120 to 1,400 μg/g (average: 800 μg/g).

In the Sangdong calcite deposit, disseminated scheelite in skarns and veins hosted in limestone formations had relatively low Nb and Nb/Ta values of 2–19 μg/g (average: 7 μg/g) and 3–19 (average: 8), respectively, as compared with the Sangdong W-Mo deposit (Figs. 10 and 11). Here, scheelite contained a smaller amount and narrower range of Sr from 20 to 73 μg/g (average: 45 μg/g); Eu anomaly values ranged from 0.64 to 53.93, and total REE concentrations from 18 to 1,200 μg/g (average: 450 μg/g). Eu anomaly values in scheelite in subeconomic prospects in the Sangdong area showed a general negative correlation with Nb concentrations and overlapped with the range and trend shown by scheelite from the Sangdong W-Mo deposit (Fig. 9).

5.3. Subeconomic Prospects in The Joongdong Area

Scheelite in the prospects of the Joongdong area generally had much lower Nb concentrations and Nb/Ta ratios than scheelite from the Sangdong W-Mo deposit. The range of Eu anomaly values was variable, but showed a slight negative correlation with Nb concentration ($y = -0.53x + 7.07$, $R^2 = 0.10$; Fig. 9). Nb concentrations in the Joongdong area were about an order of magnitude lower than those in the Sangdong deposit. Total REE concentrations (6 to 1,900 μg/g, 290 μg/g in average) were also lower than in the Sangdong W-Mo deposit.

Scheelite disseminated in the calcite-pyroxene skarns of the Sinyemi Fe-Pb-Zn deposit had Nb concentrations of 3–10 μg/g (average: 6 μg/g) and Nb/Ta ratios of 4–15 (average: 10). Sr concentrations ranged from 33 to 78 μg/g (average: 59 μg/g), Eu anomaly values from –0.30 to 1.95, and total REE concentrations from 11 to 62 μg/g (average: 34 μg/g). Disseminated scheelite in pyrrhotite-pyroxene skarns in the Imok Pb-Zn deposit had Nb and Sr compositions very similar to those in the Sinyemi deposit, but different total REE concentrations and Eu anomaly values. Scheelite in the Imok deposit had Nb concentrations of 3–12 μg/g (average: 8 μg/g), Nb/Ta ratios of 4–16 (average: 11), Sr concentrations of 28–65 μg/g (average: 35 μg/g), Eu anomaly values of 0.17–2.13, and total REE concentrations of 19–1,900 μg/g (average: 34 μg/g).

In the Samsung and Seojin calcite deposits, disseminated scheelite in pyrrhotite-pyroxene skarns contained 2–13 μg/g (average: 5 μg/g) of Nb and had a Nb/Ta of 3–9 (average: 5), which was similar to those found for Sinyemi and Imok deposits. Sr concentrations ranged from 23 to 182 μg/g (average: 52 μg/g) and were within the ranges of the Imok and Sinyemi deposits. Scheelite in the Samsung and Seojin calcite had Eu anomaly values of 0.33–9.22 and total REE concentrations of 6–540 μg/g (average: 140 μg/g).

6. DISCUSSION

The trace element chemistries of scheelites in the economic Sangdong W-Mo deposit and prospects in the Taebaeksan metallogenic region must be interpreted in the context of existing geological and petrographic information. Here, we discuss the trace element substitution of Nb and REEs in scheelite, the geochemical signature of fluid-rock interaction during scheelite deposition and magmatic-hydrothermal evolution in the Sangdong deposit and subeconomic prospects. Based on our geochemical model, we devised an exploration strategy for hidden economic scheelite orebodies in the region.

6.1. Trace Element Substitution Reactions in Scheelite

Scheelite in the Taebaeksan region contains variable amounts of the trace elements Nb, Ta, Mo, and Sr and of REEs. Stable and consistent ablation signals of trace elements (element/Ca in Fig. 7) observed by time-resolved LA-ICP-MS analyses of scheelite suggest these trace elements are incorporated into the crystal lattice of scheelite via substitution. Because of their similar ionic radii and charge valences, Mo^{6+} (59 pm; effective ionic radii) substitutes for W^{6+} (60 pm) in scheelite as a powellite ($CaMo^{6+}O_4$), whereas Sr^{2+} (118 pm) is incorporated into the Ca^{2+} (100 pm) site of scheelite (Ding et al., 2018). In the studied scheelite, we observed a strong negative correlation of Sr and Mo (Fig. 13b). This correlation might suggest a substitution of $Sr^{2+} + W^{6+} \leftrightarrow Ca^{2+} + Mo^{6+}$, although it requires information of Mo oxidation state in scheelite.

Trivalent REE ions have been suggested to substitute into scheelite in three ways: (1) by the coupled substitution of Ca by REEs and Na ($2Ca^{2+} \leftrightarrow REE^{3+} + Na^{1+}$), (2) by the coupled substitution of Ca and W by REEs and Nb ($Ca^{2+} + W^{6+} \leftrightarrow REE^{3+} + Nb^{5+}$), and (3) by the coupled substitutions of Ca by REEs and Ca vacancy ($3Ca^{2+} \leftrightarrow 2\,REE^{3+} + \square Ca$ [where $\square$ = Ca site vacancy]; (Ghaderi et al., 1999; Brugger et al., 2000; Dostal et al., 2009; Ding et al., 2018; Song et al., 2019; Su et al., 2019). Nb and Na concentrations in the Taebaeksan scheelite failed to show a positive correlation with REE concentrations, which might suggests reactions (3) could explain REE substitution in the scheelite. In the Sangdong area, some REE especially Nd concentrations show a better correlation with Nb concentrations (Fig. 14) compares to that in the Joongdong area, which might suggest that the reactions (1) as well as (3) might contribute REE substitutions in the Sangdong area. Nevertheless, only reaction (3) might explain REE substitutions in Joongdong, since Nb concentrations in magmatic-hydrothermal fluids in the Joondong area are probably poor.

6.2. Scheelite Geochemistry in The Sangdong W-Mo Deposit and Fluorescence Colors

Scheelite in the Sangdong W-Mo deposit fluoresced from yellow, white, blue-white, to blue under short-wavelength UV light (Fig. 13). The proportion of yellow fluorescence to total scheelite was relatively high (> 80%) in the central and high W-Mo grade zone of the Sangdong deposit (Fig. 5d). The fluorescence colors of scheelite represent powellite ($CaMoO_4$) fraction (Greenwood, 1943; Hsu and Galli, 1973; Tyson et al., 1988), and as previously described by Moon and Lee (1980) and Moon (1983) in ores of the Sangdong deposit. Yellow fluorescent scheelite contained the highest concentration of Mo (770 to 51,000 μg/g; average: 16,000 μg/g), whereas blue scheelite contained the lowest (0.1 to 3.2 μg/g; average: 1.3 μg/g) (Fig. 13). Although color ranges overlapped to some extent, white and blue-white fluorescence colors corresponded with intermediate Mo concentrations. Scheelite fluorescence colors also correlated with Sr concentrations:

https://doi.org/10.1007/s12303-020-0005-z

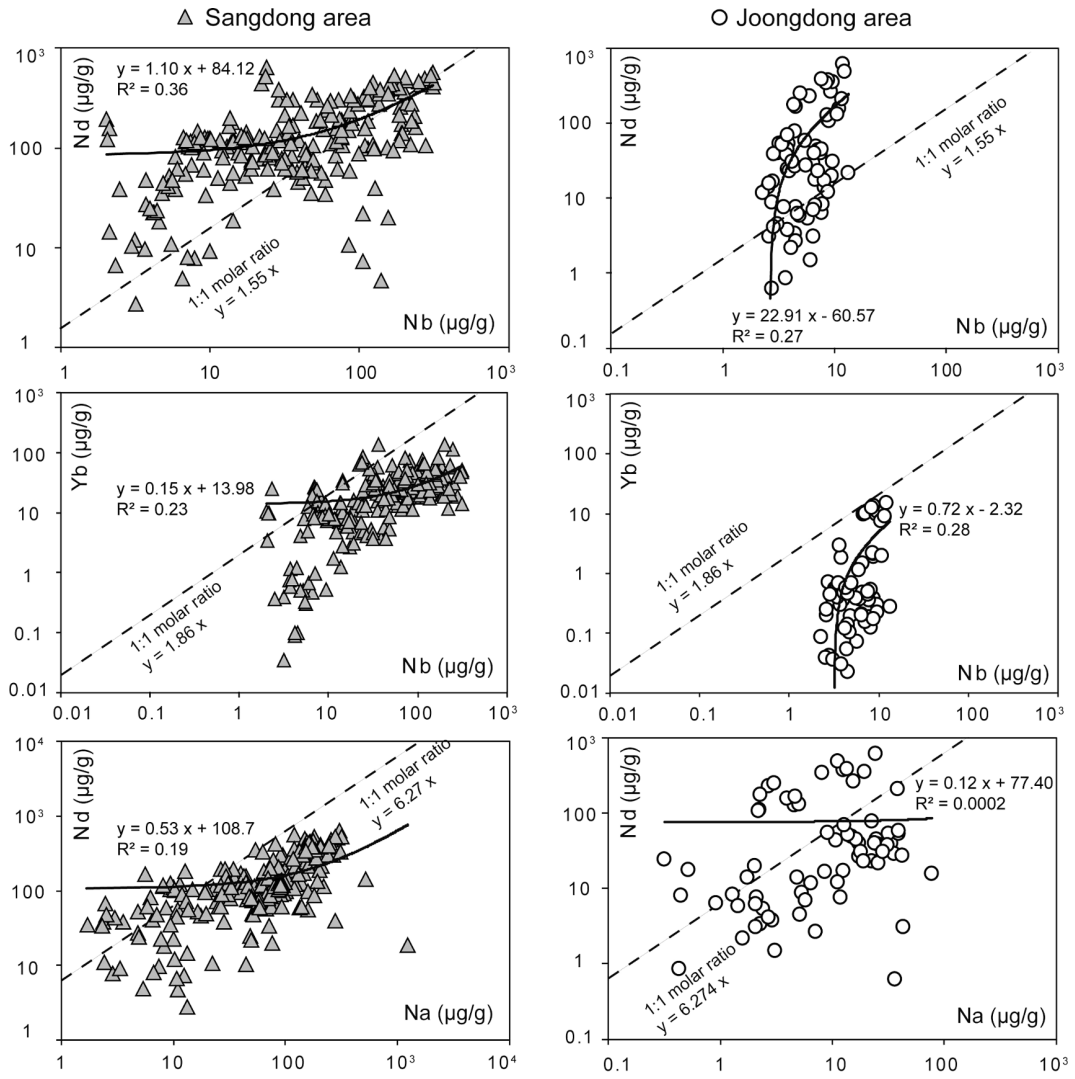

Fig. 14. Element concentration plots and linear correlative relationships between REE (Nd and Yb) versus Nb and Na in the scheelite from the Sangdong and Joongdong areas in the Taebaeksan region. The positive 1:1 molar correlation between Nb or Na and REE concentrations suggested the substitution reactions $2Ca^{2+} \leftrightarrow REE^{3+} + Na^{1+}$ and $Ca^{2+} + W^{6+} \leftrightarrow REE^{3+} + Nb^{5+}$, respectively. Nd in Sangdong scheelite show somewhat better correlations with Nb especially at higher concentrations, compared to those in the Joogdong area.

high-Sr scheelite in Sangdong W-Mo deposit fluoresced blue because it was commonly low in Mo (Fig. 13). High Mo concentrations or powellite components in scheelite could be attributed to high Mo concentrations in hydrothermal fluids and/or high Mo^{6+} concentrations in ore-forming fluids due to oxidizing hydrothermal conditions. We detected Mo concentrations of up to ~4 μg/g by microanalysis of aqueous fluid inclusions in the Sangdong deposit, and this concentration is considered to be high enough to result in economic MoS_2 mineralization (Seo et al., 2017). Although much lower than in major Mo deposits such as Questa, El Teniente, and Bingham Canyon (Klemm et al., 2007; Klemm et al., 2008; Audétat, 2010; Seo et al., 2012), Mo concentrations in hydrothermal fluids in the Sangdong W-Mo deposit (Seo et al., 2017) are greater than those in the subeconomic Mo-absent scheelites in the Joongdong area. Furthermore, the highest Ce anomaly value in scheelite were associated with the highest Mo concentration (Fig. 13), which indicates oxidizing fluids and Mo concentration in hydrothermal fluid determine Mo^{6+} concentration in scheelite.

Systematic changes in Mo and Sr contents are probably related to the extent of fluid-rock interaction during scheelite deposition. In the Sangdong deposit, the principal host for high grade W-Mo mineralization is the relatively Sr-rich carbonate layer (M1, F1, F2…) in the Myobong slate formation. Unaltered M1 limestone in the Sangdong area contains about 350 μg/g of Sr, while bulk rocks of pyroxene-garnet skarn and wollastonite-rich skarn in the same layer in the Sangdong W-Mo deposit contain variable but much less amount of Sr from 1–28 μg/g to 22 μg/g, respectively (Moon, 1983). This Sr-rich lithology reacted with a relatively oxidized and Sr-poor magmatic-hydrothermal fluid (Seo et al., 2017). High vein densities and high W-Mo grades

(John, 1963; Moon, 1983; Seo et al., 2017) occur in the central zone of the deposit, where greater fluid-rock interactions and higher ratios are expected. Higher fluid-rock ratios in the center of the intrusion would favor oxidized conditions and promote the precipitation of Mo-rich scheelite (Fig. 5). This would also explain the greater range of Sr concentrations observed in precipitated scheelite in the Sangdong deposit (Fig. 12) and higher Sr concentrations in the periphery of the deposit, which can be inferred by its blue fluorescence in the Sangdong deposit (Lee, 2001) and the negative correlation between Sr and Mo concentrations in scheelite (Fig. 13b). Because original Sr concentrations in sedimentary wallrock are the primary determinator of Sr concentrations in scheelite (Moon, 1983), the wide range of concentrations observed in scheelite from the Sangdong deposit (13–711 μg/g) suggest variable degree of fluid-rock interaction during scheelite mineralization (Fig. 12), and the large Sr concentration range in the later biotite-muscovite-quartz alteration stage might indicate greater fluid-rock interaction in this stage than in the earlier amphibole-quartz alteration stage (Fig. 12). Furthermore, the wide range of Sr concentrations observed in the Sangdong W-Mo deposit contrasted with the relatively low Sr variations found in the scheelite-bearing prospects of the Joongdong area (e.g., 33–78 μg/g in the Sinyemi, 28–65 μg/g in the Imok, and 23–182 μg/g in Seojin-Samsung calcite deposits; Fig. 12), which likely indicate limited degrees of fluid-rock interactions.

In the Sangdong W-Mo deposit, yellow fluorescence was indicative of scheelite in the higher grade, central part of the deposit, which had a greater fluid-rock ratio, whereas blue fluorescence indicated a low-grade periphery (Fig. 5d). Observed trends in the fluorescence colors of scheelite can also be applied to W exploration in the Taebaeksan metallogenic region for hidden economic scheelite orebodies with similar geochemical characters. Furthermore, blue- or blue-white fluorescent scheelites predominate in the subeconomic prospects of the Joongdong area in Taebaeksan (Figs. 6e and f), which indicates these scheelite-bearing unmineralized prospects are either subeconomic formed due to low fluid-rock ratios or the low-grade peripheral part of a hidden economic W deposit.

6.3. Geochemistry of an Economic Sangdong W-Mo Deposit and of Subeconomic Prospects in The Taebaeksan Metallogenic Region

The temporally systematic changes of Nb, Ta, and REE concentrations in the Sangdong scheelite (Figs. 9 and 11) strongly suggest that the elements are mainly originated from the magmatic-hydrothermal fluids. Oxygen isotope ratios in the quartz veins ($\delta^{18}O$ from +10 to +13‰) in the Sangdong W-Mo deposits is similar to the Sangdong granite ($\delta^{18}O$ from +10 to +11‰) (Kim et al., 1988), and bulk skarn rocks in the Sangdong W-Mo deposit and the Sangdong granite have similar REE patterns (Moon, 1989), both suggesting that the geochemistry of the deposit is dominated by the magmatic-hydrothermal fluids.

The Eu anomaly values of scheelite from the Sangdong deposit showed a broad negative correlation with Nb concentration (Fig. 9). Although the Eu anomaly values of orebodies in the Sangdong W-Mo deposit overlap with each other, paragenesis of veins and alteration assemblages in the deposit provide insight of temporal relationships during magmatic-hydrothermal fluid evolution (Fig. 9). In the main orebody, smaller Eu anomaly values were observed in the higher grade scheelite-molybdenite stage associated with quartz-biotite-muscovite alteration than in the lower grade scheelite mineralization in the earlier quartz-amphibole alteration stage. The composition and its trend of trivalent REE in the hydrothermal fluid are controlled by temperature, ligand type, and pH (Haas et al., 1995; Wood et al., 2000; Brugger et al., 2008; Migdisov et al., 2009). Moreover, Eu anomaly values and Eu^{2+}/Eu^{3+} ratios in the REE rich scheelite observed in the hydrothermal Au deposit have been suggested to be dependent on the oxidation state of the original hydrothermal fluids (Brugger et al., 2008). While both of these effects could be important, it is more likely that Eu anomaly values in Sangdong scheelite are inherited from parent magma for two reasons: (1) Eu anomaly values are correlated with Nb concentration, and (2) redox-sensitive elements like Mo are not correlated with Eu anomaly values in Sangdong scheelite (Fig. 13). Europium anomaly values and their range in scheelite from Archean hydrothermal Au deposits (Brugger et al., 2000) were not found to be correlated with Eu^{2+}/Eu^{3+} ratios calculated from XANES spectra (Brugger et al., 2008). Thus, Eu anomaly values of Taebaeksan scheelite cannot be fully explained by the oxidation state of hydrothermal fluids. Furthermore, we observed no correlation between Mo concentrations in scheelite and Eu anomaly values (Fig. 13c). Although we cannot totally rule out the effect of fluid oxidation state, we suggest that hydrothermal fluid composition is the first-order determinator of REE, Nb, and Eu anomaly values in scheelite from the Sangdong deposit.

Although correlations between Eu anomaly values or REE concentrations and Nb concentrations in magmatic-hydrothermal fluids can be controlled by multiple variables including temperature, pressure, and host lithology, the primary control variable is geochemical evolution of the causative magma. Concentrations of highly incompatible elements is strongly controlled by fractional crystallization during the final stages of magmatic evolution (Audétat and Pettke, 2003; Audetat et al., 2008; Audétat, 2010), and fractional crystallization increases Nb and REE concentrations, and the crystallization of plagioclase results in strong negative

https://doi.org/10.1007/s12303-020-0005-z

Eu anomaly values in parent magma prior to fluid exsolution. Therefore, the combined strong Eu anomaly values and increased Nb concentrations in the Sangdong W-Mo deposit are controlled by fractional crystallization of feldspar in highly fractionated parental magma. Since REEs are relatively incompatible and LREEs partition more strongly into feldspar (Larsen, 1979), fractional crystallization of feldspar and of accessory mineral phases such as zircon and rutile will control total REE concentrations and light REE/ heavy HREE ratios such as La/Yb (Fig. 11c). In the Sangdong W-Mo deposit, relatively low Eu anomaly values and low Nb concentrations in the early quartz-amphibole stage provide a signal of less fractionation, while relatively high Nb concentrations in the late quartz-biotite-muscovite stage indicate a high degree of fractionation in parent magma (Fig. 9).

Despite some scatter, scheelite from the Sangdong W-Mo deposit follows the inferred negative correlation between Eu anomaly and Nb concentration, which is referred to as the "Sangdong fractionation trend" (Fig. 9). This fractionation can also be inferred by the negative correlation between Nb and La/Yb ratios in scheelite from the Sangdong W-Mo deposit (hosted in the Myobong and lower Pungchon formations), and from the Sangdong calcite deposit (hosted in the upper sedimentary units of the upper Pungchon and the Hwajeol formations) (Fig. 11c). Relatively lower Nb, Ta, total REE concentrations, higher Eu anomaly values, and La/Yb ratios in scheelite from the Sangdong calcite deposit indicate that subeconomic scheelite in these stratigraphically upper units were formed temporally earlier than high-grade scheelite deposition in the Footwall, Main, and Hangingwall orebodies in the Sangdong W-Mo deposit (Fig. 11).

Scheelites from the Joongdong area contained Nb concentrations about an order of magnitude lower than those from the Sangdong W-Mo deposit (Fig. 9). However, both types of scheelite showed a negative correlation with the Eu anomaly values, which suggests scheelite in the Joondong area, unlike scheelite in the Sangdong W-Mo deposit, might be formed from fluids that separated from less fractionated magma. Nb/Ta ratios and La/Yb ratios in scheelite from the Sangdong W-Mo deposit and orebodies in the Joongdong area show contrasting discriminations between the economic W deposit and subeconomic prospects (Fig. 10).

The high Nb/Ta ratio observed in Sangdong scheelite may have been due to widespread hydrothermal rutile precipitation in the high-grade quartz-scheelite-molybdenite vein (Seo et al., 2017), as rutile affects the fractionation of Nb and Ta (Horng and Hess, 2000; Dostal et al., 2009). Furthermore, Ti solubility in hydrothermal fluids is significantly enhanced in F-rich fluids (Ayers et al., 1991; Ryzhenko et al., 2006; Tanis et al., 2016), which concurs with the occurrence of late fluorite in the quartz vein with muscovite alteration. Although the genetic relationship between rutile and W mineralization in Sangdong deposit is unclear, the tendency of low Nb/Ta ratios in rutile coexisting with scheelite in hydrothermal quartz veins (Dostal et al., 2009) might explain the high Nb/Ta ratios observed in scheelite from the economic Sangdong W-Mo deposit (Figs. 10 and 11d).

While subeconomic scheelites in the Joongdong area have a Nb/Ta ratio of from 3–16, the economic Sangdong W-Mo deposit has a Nb/Ta of from 11–230. If the Nb/Ta ratio of scheelite is above or below 11–16, it might be a useful discriminatory factor for evaluating economic scheelite ore deposition in the Taebaeksan metallogenic region. Blue fluorescent scheelites in the subeconomic Sunbawi veins in the Sangdong area have relatively high Nb/Ta ratios (Fig. 10), which may indicate potential for a future W exploration in the area. In addition, relatively high W concentrations in soil of the Sunbawi area also support ore potentials (Yoo, 2016). Since the fluids in the Sunbawi veins do not contain enough Ca and Fe to precipitate W minerals (Seo et al., 2017), exploration for a suitable hosting lithology in the area, such as, for limestone or Fe-rich volcanic/metamorphic rock, is essential for economic W mineralization (Polya, 1988; Lecumberri-Sanchez et al., 2017).

6.4. Geochemical Model of Scheelite Deposition in The Taebaeksan Region

Relatively lower Mo concentrations and intermediate Ce anomaly values in blue-white to white fluorescing scheelites from sub-economic prospects in the Joongdong area suggests they are either 1) peripheral to an economic W deposit or 2) part of a subeconomic (low W-grade) prospects with a low or limited degree of fluid-rock reaction (Figs. 5d, 13a, and 13b). The lower Nb values of Joongdong scheelite than of the Sangdong area (Fig. 9) suggests an association with a smaller magma reservoir that solidified before significant accumulations of ore metals, such as, W and Mo occurred, which implies studied prospects in the Joongdong area are possibly subeconomic. Nonetheless, the Sangdong deposit contains an economic scheelite ore deposit because its hydrothermal fluids are likely derived from a significantly fractionated melt possibly generated by prolonged magma fractionation in a possibly much larger magma reservoir than in the Joongdong area that accumulated ore metals before solidifying (Fig. 15). Higher alkali metal, silica, and trace elements (e.g., Rb) concentrations in Sangdong granite (Kim, 1986; Moon, 1987) also support the notion that causative magma in the Sangdong area was relatively more fractionated than granitoids in the Joongdong area (Hong, 1986; Yun, 1986; Chang et al., 1990).

Fractionation of late-stage magma in the batholith and its magmatic-hydrothermal fluids would enhance its F activities and F/Cl ratios, which concurs with the occurrence of fluorite in the late-stage Sangdong quartz vein, and probably promotes transportation of REE, Nb, and W (Audétat et al., 2000; Timo-

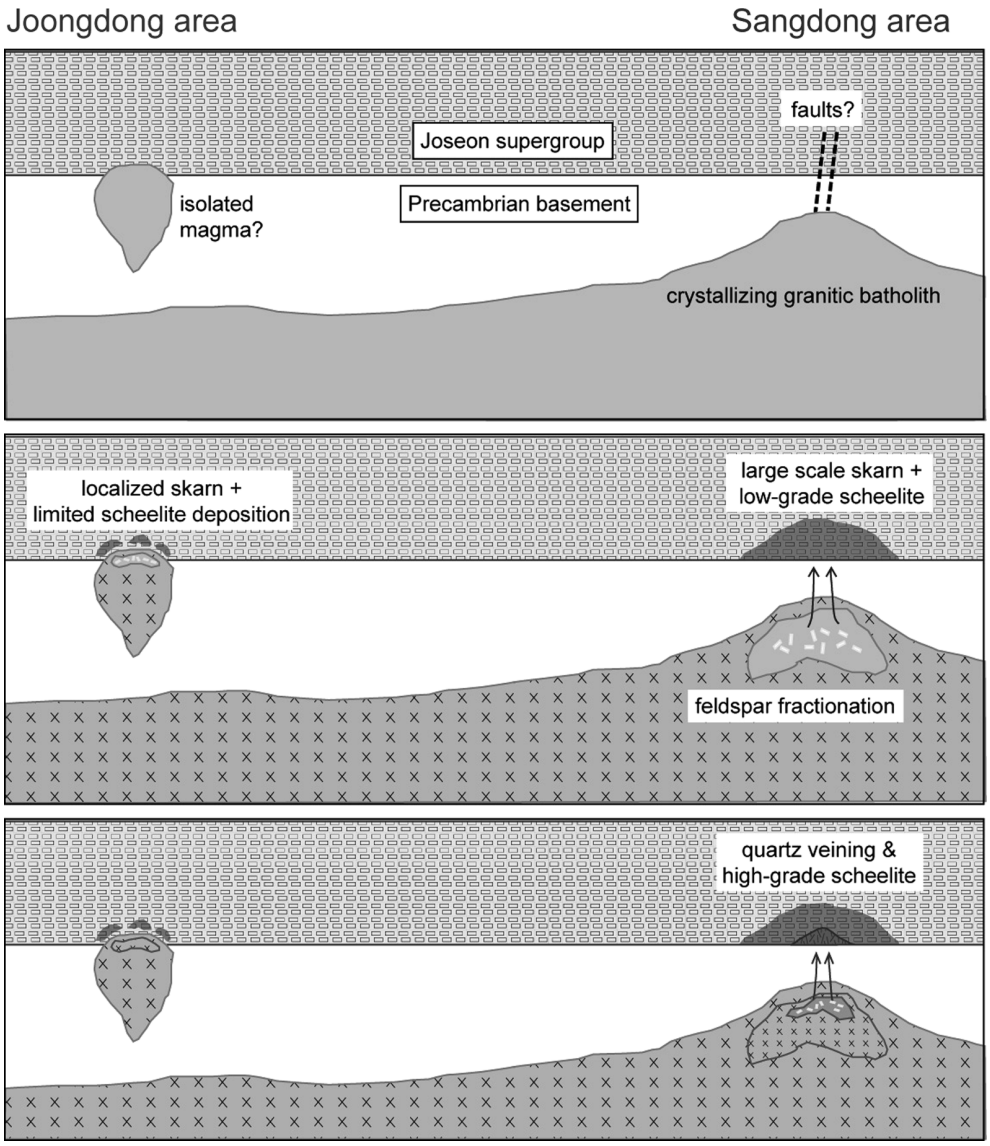

Fig. 15. Speculative geologic model of scheelite mineralization in the Joongdong and Sangdong areas in the southern Taebaeksan metallogenic region. Physically isolated magma in the Joongdong area probably has limited W potential, whereas in the Sangdong area, extensive fractionation in a larger batholith would have enabled the accumulation of incompatible elements and water and resulted in economic hydrothermal W mineralization.

feev et al., 2015; Timofeev et al., 2017). Skarn orebodies in the Joongdong area exhibit a close spatial association with local intrusive rocks (Figs. 2a, 3b, 3c, and 4b) with limited skarn propagation as compared with that observed in the Sangdong W-Mo deposit, where skarn mineralization propagates along a strike for about 1.5 km (Moon, 1984a, 1984b, 1989). In the Sinyemi Fe-Zn-Pb and Imok Zn-Pb deposits, magnetite- or pyrrhotite-bearing skarns are closely associated with the granitoid intrusions (Kim and Kim, 1978; Choi et al., 2014; Im and Shin, 2016; Yoo, 2016). Localized small-scale pyroxene-pyrrhotite skarns with disseminated scheelite developed around granitoid intrusions in the Seojin and Samsung calcite deposits (Figs. 2a and 4b).

The difference between magmatic-hydrothermal skarn propagation in the world-class Sangdong W-Mo deposit and Joongdong area is possibly due to the amount of fluids derived from causative magma (Fig. 15). Smaller granitic intrusions in the Joongdong area with a relatively low water content and limited degree of fractionation (Lee et al., 1996b) would produce localized skarn bodies of subeconomic scheelite grades as found in the outcrop (Fig. 4b). Granitoid magmas in the Joongdong area may have been physically separated from a larger-scale batholithic magma reservoir prior to water saturation. Two major N-S trending strike-slip faults passing through the Sangdong area (Fig. 5a) may have provided an effective conduit for the magmatic-hydrothermal fluids required to form economic scheelite mineralization. The high vein density zone in the Sangdong W-

https://doi.org/10.1007/s12303-020-0005-z

Mo deposit (John, 1963) coincides with the zone between the two major faults. Moreover, a highly fractured zone with small-scale magnetite-pyrrhotite skarn orebodies with disseminated scheelite occurs between faults in the Sangdong calcite deposit. Although more further studies including fluid inclusions, structural geology, isotope geochemistry, geochemical exploration, and alteration mineralogy are required to fully understand scheelite mineralization processes in the Taebaeksan metallogenic region, scheelite geochemistry suggests that there is relatively low potential for economic scheelite mineralization in the Joondong area.

7. CONCLUSIONS

Base on scheelite geochemistries in the Sangdong W-Mo deposit and in the sub-economic unmineralized prospects of the southern Taebaeksan metallogenic region, we derived the following conclusions:

(1) In the Taebaeksan region, scheelite fluorescence colors, strongly related with the powellite ($CaMoO_4$) fraction, correlate as well with scheelite Sr concentrations, which might be related to degrees of fluid-rock interaction. This suggests that the fluorescence color of scheelite might provide a useful means of evaluating degree of fluid-rock interaction and an explorative tool in the southern Taebaeksan region.

(2) In the Taebaeksan region, the negative correlation between Nb concentration and Eu anomaly in scheelite is probably determined by degree of fractional crystallization and possibly by the size of causative magma. Low Nb and REE concentrations in disseminated scheelite from subeconomic prospects in the Joongdong area suggest a relatively less fractionated magma physically separated from a batholith-scale magma chamber.

(3) In the Taebaeksan metallogenic region, scheelite Nb/Ta ratios differentiated sub-economic scheelite in the Joongdong area (3–16) and an economic scheelite orebody in the Sangdong W-Mo deposit (11–230), which suggests Nb/Ta ratios may be useful for mineral exploration in this region.

ACKNOWLEDGMENTS

We thank Dr. Markus Walle for his assistance with the LA-ICP-MS analysis in ETH Zurich and Ms. Seunghee Han in Korea Polar Research Institute (KOPRI). This work was supported by a National Research Foundation (NRF) of Korea grant funded by the Korean government (MSIT) (#NRF-2019R1C1C1002588) and by the Korea Institute for Geoscience and Mineral Resources (KIGAM) research projects "Geology and ore deposit survey and origin study for securing potential orebodies in the Taebaegsan metallogenic belt" (15-3211 and 16-3211) and "Verification of North Korean mineral resources exploration technologies and potential evaluation of North Korean mineral deposits" (18-8901 and 19-8901). Staff from the Sangdong deposit (Almonty Korea) and calcite deposits (Omya Korea) are thanked for their assistance with underground and drill core sampling. We thank Dr. Dominique Tanner and Dr. Johann Raith for constructive discussion.

REFERENCES

Anders, E. and Grevesse, N., 1989, Abundances of the elements: meteoritic and solar. Geochimica et Cosmochimica Acta, 53, 197–214.

Audétat, A., 2010, Source and evolution of molybdenum in the porphyry Mo(-Nb) deposit at Cave Peak, Texas. Journal of Petrology, 51, 1739–1760.

Audétat, A. and Pettke, T., 2003, The magmatic-hydrothermal evolution of two barren granites: a melt and fluid inclusion study of the Rito del Medio and Canada Pinabete plutons in northern New Mexico (USA). Geochimica et Cosmochimica Acta, 67, 97–121.

Audétat, A., Günther, D., and Heinrich, C.A., 2000, Causes for large-scale metal zonation around mineralized plutons: fluid inclusion LA-ICP-MS evidence from the Mole Granite, Australia. Economic Geology, 95, 1563–1581.

Audétat, A., Pettke, T., Heinrich, C.A., and Bodnar, R.J., 2008, The composition of magmatic-hydrothermal fluids in barren and mineralized intrusions. Economic Geology, 103, 877–908.

Ayers, J.C., Watson, E.B., Tarney, J., Pickering, K.T., Knipe, R.J., and Dewey, J.F., 1991, Solubility of apatite, monazite, zircon, and rutile in supercritical aqueous fluids with implications for subduction zone geochemistry. Philosophical Transactions of the Royal Society of London, Series A: Physical and Engineering Sciences, 335, 365–375.

Barton, M.D., 1987, Lithophile-element mineralization associated with Late Cretaceous two-mica granites in the Great Basin. Geology, 15, 337–340.

Brugger, J., Lahaye, Y., Costa, S., Lambert, D., and Bateman, R., 2000, Inhomogeneous distribution of REE in scheelite and dynamics of Archaean hydrothermal systems (Mt. Charlotte and Drysdal gold deposits, Western Australia). Contributions to Mineralogy and Petrology, 139, 251–264.

Brugger, J., Etschmann, B., Pownceby, M., Liu, W., Grundler, P., and Brewe, D., 2008, Oxidation state of europium in scheelite: tracking fluid-rock interaction in gold deposit. Chemical Geology, 257, 26–33.

Chang, H.W., Lee, M.S., and Cho, D.J., 1990, Comparison of geocehmical characteristics of the Shinyemi granite and the Imog granite, northeastern part of South Korea. Journal of the Geological Society of Korea, 4, 313–323.

Chang, H.W., Cheong, C.S., Park, H.I., and Chang, B.U., 1995, Lead isotopic study on the Dongnam Fe-Mo skarn deposit. Economic and Environmental Geology, 28, 25–31.

Chi, S.J., 2011, Evaluation of development possibility for the security of industrial mineral resources (Cu, Pb, Zn, Au etc) on the domestic mines. Report GP2010-024-2011(2), Korea Institute of Geoscience and Mineral Resource (KIGAM), Daejeon, 351 p.

Choi, D.K., 1998, The Yongwol Group (Cambrian–Ordovician) redefined: a proposal for the stratigraphic nomenclature of the Choson

Supergroup. Geosciences Journal, 2, 220–234.
Choi, E., Choi, S.G., Seo, J., Kim, C.S., and Park, S.G., 2014, Geology, mineralogy and geochemistry of the Shinyemi iron deposit, Korea: implications for a genetic model. Acta Geologica Sinica, 88, 1083–1084.
Choi, S.G., Choi, B.K., Ahn, Y.H., and Kim, T.H., 2009, Re-evaluation of genetic environments of zinc-lead deposits to predict hidden skarn orebody. Economic and Environmental Geology, 42, 301–314.
Ding, T., Ma, D., Lu, J., and Zhang, R., 2018, Garnet and scheelite as indicators of multi-stage tungsten mineralization in the Huangshaping deposit, southern Hunan province, China. Ore Geology Reviews, 94, 193–211.
Dostal, J., Kontak, D.J., and Chatterjee, A.K., 2009, Trace elements geochemistry of scheelite and rutile from metaturbidite-hosted quartz vein gold deposits, Meguma Terrane, Nova Scotia, Canada: geneti implications. Mineralogy and Petrology, 97, 95–109.
Farrar, E., Clark, A.H., and Kim, O.J., 1978, Age of the Sangdong tungsten deposit, Republic of Korea, and its bearing on the metallogeny of the Southern Korean Peninsula. Economic Geology, 73, 547–552.
Fu, Y., Sun, X., Zou, H., Lin, H., Jiang, L., and Yang, T., 2017, In-situ LA-ICP-MS trace elements analysis of scheelites from the giant Beiya gold-polymetallic deposit in Yunnan Province, Southwest China and its metallogenic implications. Ore Geology Reviews, 80, 828–837.
Gaudette, H.E. and Hurley, P.M., 1973, U-Pb zircon age of Precambrian basement gneiss of South Korea. Geological Society of America Bulletin, 84, 2305–2506.
Ghaderi, M., Michael Palin, J., Campbell, I.H., and Sylvester, P.J., 1999, Rare earth element systematics in scheelite from hydrothermla gold deposits in the Kalgoorlie–Norseman region, Western Australia. Economic Geology, 94, 423–438.
Gliddon, J., Gribble, P., Carter, A., Elvish, R., Thomas, P., Turner, M., Liukko, G., Jansons, K., and Wrigley, T., 2012, Sangdong project feasibility study. Report, Document No. 1053410100-REP-R0002-01, Wardrop, Swindon, UK, 230 p. https://secure.kaiserresearch.com/i/jk/tr16/TRWOF20120602.pdf
Go, G.H., 1986, Study on mineralization and skarn minerals of the Sangdong tungsten deposit. MSc. Thesis, Ewah Womans University, Seoul, Korea, 50 p. http://dspace.ewha.ac.kr/handle/2015.oak/196790
Greenwood, R., 1943, Effect of chemical impurities on scheelite fluorescence. Economic Geology, 38, 56–64.
Guillong, M., Meier, D.L., Allan, M.M., Heinrich, C.A., and Yardley, B.W.D., 2008, SILLS: a MATLAB-based program for the reduction of laser abalation ICP-MS data of homogeneous materials and inclusions. In: Sylvester, P. (ed.), Laser Ablation ICP-MS in the Earth Sciences: Current Practices and Outstanding Issues. Mineralogical Association of Canada Short Course, Québec, 40, p. 328–333.
Guo, S., Chen, Y., Liu, C.Z., Wang, J.G., Su, B., Gao, Y.J., Wu, F.Y., Sein, K., Yang, Y.H., and Mao, Q., 2016, Scheelite and coexisting F-rich zoned garnet, vesuvianitem fluoritem and apatite in calc-silicate rocks from the Mogok metamorphic best, Myanmar: implications for metasomatism in marble and the role of halogens in W mobilization and mineralization. Journal of Asian Earth Sciences, 117, 82–106.
Haas, J.R., Shock, E.L., and Sassani, D.C., 1995, Rare earth elements in hydrothermal systems: estimates of standard partial molal thermodynamic properties of aqueous complexes of the rare earth elements at high pressures and temperatures. Geochimica et Cosmochimica Acta, 59, 4329–4350.
Hong, Y.K., 1986, Geochemistry and K-Ar age of the Imog granite at the southwestern part of the Hambaeg basin, Korea. Economic and Environmental Geology, 19, 07–107.
Horng, W.S. and Hess, P.C., 2000, Partition coefficients of Nb and Ta between rutile and anhydrous haplogranite melts. Contributions to Mineralogy and Petrology, 138, 176–185.
Hsu, L.C. and Galli, P.E., 1973, Origin of the scheelite-powellite series of minerals. Economic Geology, 68, 681–696.
Huang, L.C. and Jiang, S.Y., 2014, Highly fractionated S-type granites from the giant Dahutang tungsten deposit in Jiangnan Orogen, Southest China: geochronology, petrogenesis and their relationship with W-mineralization. Lithos, 202–203, 207–226.
Hwang, D.H. and Lee, J.Y., 1998, Ore genesis of the Wondong polymetallic mineral deposits in the Taebaegsan metallogenic province. Economic and Environmental Geology, 31, 375–388.
Im, H. and Shin, D., 2016, Mineral composition and genetic environmental of skarn and hydrothermal vein type ore bodies in Imog deposit. Proceedings of the Fall Joint Conference of the Geological Science in Korea, Pyeongchang, Korea, Oct. 24–27, p. 226.
John, Y.W., 1963, Geology and origin of Sandong tungsten mine, Republic of Korea. Economic Geology, 58, 1285–1300.
Kim, C.S., Choi, S.G., Kim, G.B., Kang, J., Kim, K.B., Kim, H., Lee, J., and Ryu, I.C., 2017, Genetic environments of the high-purity limestone in the upper zone of the Daegi Formation at the Jeongseon–Samcheok area. Economic and Environmental Geology, 50, 287–302.
Kim, E.J., Park, M.E., and White, N.C., 2012, Skarn gold mineralization at the Geodo mine, South Korea. Economic Geology, 107, 537–551.
Kim, J.H. and Lee, K.M., 2000, Report of detailed survey: limestone, the Jeongseon–Yemi area. Report, Korea Mineral Resource Corporation (KORES), Seoul, 73 p.
Kim, K., 1986, Petrology and petrochemistry of Sangdong granite. M.Sc. Thesis, Kyungpook National University, Daegu, Korea, 80 p.
Kim, K.H. and Nakai, N., 1982, Sulfur isotope composition and isotopic temperatures of the Shinyemi lead and zinc ore deposits, western Taebaegsan Metallogenic Belt, Korea. Economic and Environmental Geology, 15, 156–166.
Kim, K.H. and Shin, Y.H., 1995, Nd-Sr isotope and gas composition for the Sangdong Granites related to the tungsten-molybdenum ore mineraliztion. Economic and Environmental Geology, 28, 139–145.
Kim, K.H., Nakai, N., and Kim, O.J., 1981, A mineralogical study of the skarn minerals from the Shinyemi lead-zinc ore deposits, Korea. Economic and Environmental Geology, 14, 167–182.
Kim, K.H., Kim, O.J., Nakai, N., and Lee, H.J., 1988, Stable isotope studies of the Sangdong tungsten ore deposit, South Korea. Mining Geology, 38, 473–487. https://doi.org/10.11456/shigenchishitsu1951.38.473
Kim, O.J. and Kim, K.H., 1978, On the genesis of the ore deposits of Yemi district in the Taebaeksan Metallogenic Province. Journal of Natural Science Institute, Yonsei University, Seoul, 2, 71–94.
Klemm, L.M., Pettke, T., and Heinrich, C.A., 2008, Fluid and source magma evolution of the Questa porphyry Mo deposit, New Mexico, USA. Mineralium Deposita, 43, 533–552.

https://doi.org/10.1007/s12303-020-0005-z

Klemm, L.M., Pettke, T., Heinrich, C.A., and Campos, E., 2007, Hydrothermal evolution of the El Teniente deposit, Chile: porphyry Cu-Mo ore deposition from low-salinity magmatic fluids. Economic Geology, 102, 1021–1045.

Koh, Y.K., Choi, S.G., So, C.S., Choi, S.H., and Uchida, E., 1992, Application of arsenopyrite geothermometry and sphalerite geobarometry to the Taebaek Pb-Zn(-Ag) deposit at Yeonhwa I mine, Republic of Korea. Mineralium Deposita, 27, 58–65.

Larsen, L.M., 1979, Distribution of REE and other trace elements between phenocrysts and peralkaline undersaturated magmas, exemplified by rocks from the Gardar igneous province, south Greenland. Lithos, 12, 303–315.

Lecumberri-Sanchez, P., Vieira, R., Heinrich, C.A., Pinto, F., and Walle, M., 2017, Fluid-rock interaction is decisive for the formation of tungsten deposit. Geology, 45, 579–582.

Lee, C.H., Lee, H.K., and Kim, S.J., 1998, Geochemistry and mineralization age of magnesian skarn-type iron deposits of the Janggun mine, Republic of Korea. Mineralium Deposita, 33, 379–390.

Lee, H.J., 2001, Report on Sangdong tungsten mine in Korea. Report, Korea Engineering Co. Ltd., Seoul, 45 p.

Lee, H.K., 2016, Lead isotopic compositions of sphalerite in the Taebaeksan region. Report, Korea Institute of Geoscience and Mineral Resource (KIGAM), Daejeon, 237 p.

Lee, H.K., Ko, S.J., and Imai, N., 1990, Genesis of the lead-zinc-silver and iron deposits of the Janggun mine, as related to their structural features: structural control and wallrock alteration of ore formation. Economic and Environmental Geology, 23, 161–181.

Lee, H.K., Lee, C.H., and Kim, S.J., 1996a, Geochemistry of stable isotope and mineralization age of magnetite deposits from the Janggun mine, Korea. Economic and Environmental Geology, 29, 411–419.

Lee, H.K., Moon, H.S., and Oh, M.S., 2007, Economic mineral deposits in Korea. ACANET, Seoul, 762 p.

Lee, J.H., 2018, Sphalerite geochemistry of Zn-Pb orebodies in the Taebaeksan metallogenic belt. M.Sc. Thesis, Inha University, Incheon, Korea, 88 p.

Lee, J.H., Yoo, B.C., Yang, Y., Lee, T.H., and Seo, J.H., 2019, Sphalerite geochemistry of the Zn-Pb orebodies in the Taebaeksan metallogenic province, Korea. Ore Geology Reviews, 107, 1046–1067.

Lee, J.Y., Lee, I.H., and Hwang, D.H., 1996b, Chemical composition of the Cretaceous granitoids and related ore deposits in the Taebaegsan basin, Korea. Economic and Environmental Geology, 29, 247–256.

Lee, Y.I. and Lee, J.I., 2003, Paleozoic sedimentation and tectonics in Korea: a review. Island Arc, 12, 162–179.

Migdisov, A.A., Williams-Jones, A.E., and Wagner, T., 2009, An experimental study of the solubility and speciation of the rare earth elements (III) in fluoride- and chloride-bearing aqueous solutions at temperatures up to 300 °C. Geochimica et Cosmochimica Acta, 73, 7087–7109.

Moon, K.J., 1983, The genesis of the Sangdong tungsten deposit, the republic of Korea. Ph.D. Thesis, University of Tasmania, Australia, 366 p.

Moon, K.J., 1984a, Condition of the Sangdong tungsten skarn formation. Economic and Environmental Geology, 17, 259–272.

Moon, K.J., 1984b, Stable isotope study on the Sangdong deposit. Economic and Environmental Geology, 17, 171–177.

Moon, K.J., 1985, Fluid inclusion study of the Sangdong tungsten skarn deposits. Economic and Environmental Geology, 18, 205–216.

Moon, K.J., 1986, Comparison study of geochemistry of the Sangdong skarn orebody in a large scale and small scale. Economic and Environmental Geology, 19, 113–119.

Moon, K.J., 1987, Significance of the occurences of the Sangdong Granite and scheelite-bearing quartz veins in the Precambrian schist. Journal of the Geological Society of Korea, 23, 306–316.

Moon, K.J., 1989, REE patterns at the Sangdong tungsten skarn ore deposit, South Korea. Journal of the Geological Society of Korea, 25, 205–215.

Moon, K.J., 1991a, Review of skarn ore deposits at the southern limb of the Baegunsan syncline in the Taebaeg basin of South Korea. Journal of the Geological Society of Korea, 27, 271–292.

Moon, K.J., 1991b, Application of fluid inclusions in mineral exploration. Journal of Geochemical Exploration, 42, 205–221.

Moon, K.J. and Lee, H.J., 1980, A study on the melybdenum in scheelite of Sangdong tungsten orebodies. Economic and Environmental Geology, 13, 117–127.

Newberry, R.J., 1982, Tungsten-bearing skarns of the Sierra Nevada. I. The Pine Creek mine, California. Economic Geology, 77, 823–844.

Noh, J.H. and Oh, S.J., 2005, Hydrothermal alteration of the Pungchon limestone and the formation of high-Ca limestone. Journal of the Geological Society of Korea, 41, 175–197.

Park, C., Song, Y., Chi, S.J., Kang, I.M., Yi, K., and Chung, D., 2013, U-Pb (SHRIMP) and K-Ar age dating of intrusive rocks and skarn minerals at the W-skarn in Weondong deposit. Journal of Mineralogical Society of Korea, 26, 161–174.

Park, C., Song, Y., Kang, I.M., Shim, J., Chung, D., and Park, C.S., 2017b, Metasomatic changes during periodic fluid flux recorded in grandite garnet from the Weondong W-skarn deposit, South Korea. Chemical Geology, 451, 135–153.

Park, C., Choi, W., Kim, H., Park, M.H., Kang, I.M., Lee, H.S., and Song, Y., 2017a, Oscillatory zoning in skarn garnet: implications for tungsten ore exploration. Ore Geology Reviews, 89, 1006–1018.

Park, H.I., Chang, H.W., and Jin, M.S., 1988, K-Ar ages of mineral deposits in the Taebaeg mountain district. Economic and Environmental Geology, 21, 57–67.

Park, K.H. and Chang, H.W., 2005, Pb isotopic composition of Yeonhwa and Janggun Pb-Zn ore deposits and origin of Pb: role of Precambrian crustal basement and Mesozoic igneous rocks. Journal of Petrological Society of Korea, 14, 141–148.

Park, K.H., Cheong, C.S., Lee, K.S., and Chang, H.W., 1993, Isotopic composition of lead in Precambrian granitic rocks of the Taebaeg area. Journal of the Petrological Society of Korea, 29, 387–395.

Polya, D.A., 1988, Efficiency of hydrothermal ore formation and the Panasqueira W-Cu(Ag)-Sn vein deposit. Nature, 333, 838.

Ryzhenko, B.N., Kovalenko, N.I., and Prisyagina, N.I., 2006, Titanium complexation in hydrothermal systems. Geochemistry International, 44, 879–895.

Sato, K., Shibata, K., Uchiumi, S., and Shimazaki, H., 1981, Mineralization age of the Shinyemi Zn-Pb-Mo deposit in the Taebaegsan area, southern Korea. Mining Geology, 31, 333–336. https://doi.org/10.11456/shigenchishitsu1951.31.333

Seo, J., Choi, S.G., Kim, C.S., Park, J.W., Yoo, I.K., and Kim, N.H., 2007, The skarnification and Fe-Mo mineralization at lower part of western Shinyemi orebody in Taeback area. Journal of Mineralogical Society of Korea, 20, 35–46.

Seo, J.H., Guillong, M., and Heinrich, C.A., 2012, Separation of molybdenum and copper in porphyry deposits: the roles of sulfur, redox and pH in ore mineral deposition at Bingham Canyon. Economic Geology, 107, 333–356.

Seo, J.H., Yoo, B.C., Villa, I.M., Lee, J.H., Lee, T.H., Kim, C.S., and Moon, K.J., 2017, Magmatic-hydrothermal processes in Sangdong W-Mo deposit, Korea: study of fluid inclusions and ^{39}Ar-^{40}Ar geochronology. Ore Geology Reviews, 91, 316–334.

So, C.S., Yun, S.T., and Koh, Y.K., 1993, Mineralogic, fluid inclusion, and stable isotope evidence for the genesis of carbonate-hosted Pb-Zn(-Ag) orebodies of the Taebaek Deposit, Republic of Korea. Economic Geology, 88, 855–872.

Song, G.X., Cook, N.J., Li, G.M., Qin, K.Z., Ciobanu, C.L., Yang, Y.H., and Xu, Y.X., 2019, Scheelite geochemistry in porphyry-skarn W-Mo systems: a case study from the Gaojiabang Deposit, East China. Ore Geology Reviews, 113, 103084. https://doi.org/10.1016/j.oregeorev.2019.103084

Su, S.Q., Qin, K.Z., Li, G.M., Olin, P. and Thompson, J., 2019, Cathodoluminescence and trace elements of scheelite: Constraints on ore-forming processes of the Dabaoshan porphyry Mo-W deposit, South China. Ore Geology Reviews, 113, 103084. https://doi.org/10.1016/j.oregeorev.2019.103084

Sylvester, P.J. and Ghaderi, M., 1997, Trace element analysis of scheelite by excimer laser ablation-inductively coupled plasma-mass spectrometry (ELA-ICP-MS) using a synthetic silicate glass standard. Chemical Geology, 141, 49–65.

Tanis, E.A., Simon, A., Zhang, Y., Chow, P., Xiao, Y., Hanchar, J.M., Tschauner, O., and Shen, G., 2016, Rutile solubility in NaF-NaCl-KCl-bearing aqueous fluids at 0.5–2.79 GPa and 250–650 °C. Geochimica et Cosmochimica Acta, 177, 170–181.

Timofeev, A., Migdisov, A.A., and Williams-Jones, A.E., 2015, An experimental study of the solubility and speciation of niobium in fluoride-bearing aqueous solutions at elevated temperature. Geochimica et Cosmochimica Acta, 158, 103–111.

Timofeev, A., Migdisov, A.A., and Williams-Jones, A.E., 2017, An experimental study of the solubility and speciation of tantalum in fluoride-bearing aqueous solutions at elevated temperature. Geochimica et Cosmochimica Acta, 197, 294–304.

Tyson, R.M., Hemphill, W.R., and Theisen, A.F., 1988, Effect of the W:Mo ratio on the shift of excitation and emission spectra in the scheelite-powellite series. American Mineralogist, 73, 1145–1154.

Wheeler, A., 2016, Technical report on the mineral resources and reserves of the Sangdong project, South Korea. Report NI 43-101, Almonty Industries, Toronto, Canada, 253 p.

Wood, S.A., Wesolowski, D.J., and Palmer, D.A., 2000, The aqueous geochemistry of the rare earth elements: IX. A potentiometric study of Nd^{3+} complexation with acetate in 0.1 molal NaCl solution from 25 to 250 °C. Chemical Geology, 167, 231–253.

Yang, D.Y., 1991, Mineralogy, petrology and geochemistry of the magnesian skarn-type magnetite deposits at the Shinyemi mine, Republic of Korea. Ph.D. Thesis, Waseda University, Tokyo, 323 p.

Yoo, B.C., 2012, Element dispersion by the wallrock alteration of Janggun lead-zinc-silver deposit. Economic and Environmental Geology, 45, 623–641.

Yoo, B.C., 2016, Geology and ore deposit survey, and origin study for securing potential orebody in the Taebaegsan metallogenic belt. Report GP2015-032-2015(1), Korea Institute of Geoscience and Mineral Resource (KIGAM), Daejeon, 237 p.

Yoon, G.S., Yoon, W.S., Kim, I.S., Jeong, E.J., Yoon, M.J., Lee, J.T., Lim, B.R., Oh, Y.B., Lim, S.T., Moon, K.H., and Kim, J.H., 2013, Detailed exploration report of Seobyuk W area. Report, Korea Mineral Resource Corporation (KORES), Seoul, 120 p.

Yun, H.S., 1986, Petrochemical study on the Cretaceous granitic rocks in the southern area of Hambaeg basin. Economic and Environmental Geology, 19, 175–191.

Yun, H.S., 1988, Metamorphic facies of Goseonri Formation and petrogenetic comparison of granitic rocks in the Sangdong area. Journal of the Geological Society of Korea, 24, 189–198.

Yun, S., 1983, Skarn-ore associations and phase equilibria in the Yeonhwa-Keodo mines, Korea. Economic and Environmental Geology, 16, 1–10.

Yun, S. and Silberman, M.L., 1979, K-Ar geochronology of igneous rocks in the Yeonhwa-Ulchin zinc-lead district and southern margin of the Taebaegsan basin, Korea. Journal of the Geological Society of Korea, 15, 89–100.

Yun, S. and Einaudi, M.T., 1982, Zinc-lead skarns of the Yeonhwa-Ulchin district, South Korea. Economic Geology, 77, 1013–1032.

https://doi.org/10.1007/s12303-020-0005-z